THESIS

QUANTIFYING THE IMPACT OF CLIMATE EXTREMES ON SALT MOBILIZATION AND LOADING IN NON-DEVELOPED, HIGH-DESERT LANDSCAPES

Submitted by

Eleanor Henson

Department of Civil and Environmental Engineering

In partial fulfillment of the requirements

For the Degree of Master of Science

Colorado State University

Fort Collins, Colorado

Summer 2022

Master's Committee:

Advisor: Ryan Bailey

Ryan Morrison
Stephen Leisz

Copyright by Eleanor Henson 2022

All Rights Reserved

ABSTRACT

QUANTIFYING THE IMPACT OF CLIMATE EXTREMES ON SALT MOBILIZATION AND LOADING IN NON-DEVELOPED, HIGH-DESERT LANDSCAPES

Excess salt loading acts as a chemical stressor in water bodies and can have significant impacts on water quality. High salinity threatens sustainable crop production globally and is especially prevalent in semi-arid and arid regions. For this reason, salt transport in irrigated semi-arid and arid regions has been intensively studied. However, comparatively little research has been conducted to evaluate the salinity contributions of dominantly non-irrigated basins, and to my knowledge, no previous research has evaluated the changes in salt loads from upland semi-arid catchments in the face of climate change and extreme climate events.

This research utilizes the Soil and Water Assessment Tool (SWAT) and a coupled salinity module (SWAT-Salt), applied to a natural watershed, to fill this knowledge gap. SWAT-Salt simulates the reactive transport of 8 major salt ions, SO_4^{2-}, Cl^-, CO_3^{2-}, HCO_3^-, Ca^{2+}, Na^+, Mg^{2+}, and K^+, in the soil-aquifer-stream system of a watershed, with salt mass transported via major hydrologic pathways (surface runoff, percolation, recharge, soil lateral flow, upflux, and groundwater discharge). Specifically, this study has two major research objectives: 1) develop an accurate SWAT-Salt model that can estimate salinity loads from a largely undeveloped, upland desert catchment, the Purgatoire River Basin in Colorado, USA; and 2) quantify changes in predicted salt loads in the Purgatoire River Basin with increasing storm intensity.

The SWAT-Salt model developed in this study was used to evaluate the contribution of salt to the Arkansas River from the Purgatoire River, a dominantly non-irrigated desert catchment in southeastern Colorado. The ~8,935 km^2 Purgatoire River basin is susceptible to high salt transport due to very high topographic slopes, dry climatic conditions, and sparse vegetation. Much of the natural salt in this region has been deposited from 20,000 years of weathering the Mancos Shale formation. Calibration and validation of the salinity module was evaluated through comparisons of measured and simulated in-stream loads of individual salt ions during the period 1990-2010. Model results indicate that 76% of the salt in the Purgatoire River comes from groundwater sources, and ~24% of the salt comes from landscape soil lateral flow. Sulfate, calcium, and bicarbonate account for ~56%, ~20%, and 14% of the total salt load, respectively. The impact of climate change on salt transport and mobilization was evaluated through model scenarios of increasing storm intensity (5% and 35% increases in daily precipitation for the most extreme storms) congruent with global climate models.

Results suggest that if the largest storm events increase in intensity by the maximum predicted value of 35%, the total salt mass exported from the Purgatoire River watershed would increase by 73%. If the largest storm events increase in intensity by the median predicted value of 5%, the total salt mass exported would increase by 12%. Similar results are expected but should be evaluated for other upland desert catchments. From this thesis, I conclude that: 1) natural, largely undeveloped basins can export significant salt loads to downstream agricultural regions; 2) Future increasing storm intensity with changing climatic conditions can have a large impact on salt exports from high-desert landscapes; and 3) process-based models such as SWAT-Salt can be valuable in evaluating salt loadings from high-desert watersheds and can be applied to other watersheds worldwide.

ACKNOWLEDGEMENTS

I am very grateful for the experiences gained while working on my master's thesis at Colorado State University, and this work would not have been possible without the help from many people along the way. First, thank you, Dr. Bailey, for all your guidance. I consider myself lucky to have found such an encouraging, helpful, and motivating advisor to work with. Thank you to my lab mates, Carly Zimmer, Soheil Nozari, and Liz Motter, for your support and assistance in data collection, SWAT modeling techniques, and Python coding. Thank you to Dr. Morrison and Dr. Leisz for agreeing to be on my thesis committee and for teaching fascinating courses during my master's career. I greatly appreciate all the professors that have inspired me here at Colorado State University. Thank you to my friends and family that have steadfastly encouraged me during this journey. I am forever grateful for your love and support. Lastly, I appreciate the funding from the National Science Foundation and their continued support of research focused on protecting the quality of our nation's water resources.

TABLE OF CONTENTS

LIST OF TABLES

LIST OF FIGURES

1. INTRODUCTION

1.1 Salinity in Watersheds

Salinization is a global concern for the degradation of soil and water resources. Excess salt minerals can decrease water quality, cause biodiversity loss, decrease crop yield, increase risk of soil erosion, contaminate drinking water, and lower soil biological activity (Vengosh, 2014; Zamann et al., 2018). Soluble salt ions, such as sodium (Na^+), calcium (Ca^{2+}), magnesium (Mg^{2+}), sulfate (SO_4^{2-}), potassium (K^+), chloride (Cl^-), carbonate (CO_3^{2-}), and bicarbonate (HCO_3^-), can be deposited in soil and water supplies both naturally and anthropogenically.

Natural salt deposits can accumulate from parent rock or soil material with salt minerals dissolving to mobile ions (e.g. gypsum, $CaSO_4$, dissolving to Ca^{2+} and SO_4^{2-}). These mobile ions are then transported via hydrologic pathways to surface water streams and reservoirs, soil water, and groundwater supplies (Burkhalter et al., 2006). This is particularly a concern in regions with shallow water tables, low soil permeability, high evapotranspiration, and sparse precipitation (Hassani et al., 2020; Hosseini & Bailey, 2022). Anthropogenic actions that can increase salinization include vegetation clearing, mining activities, application of road salts (Dugan et al., 2017), and effluent from wastewater treatment plants, but the most prominent human act that leads to increased salinization is irrigation, specifically in semi-arid regions. Sharp declines in crop production have occurred in 27%-28% of irrigated land in the western United States due to high soil salinity, which prevents root water uptake and inhibiting transpiration and photosynthetic processes (Bailey et al., 2019; Tanji, 2004), with high soil salinity occurring due to salt mineral dissolution, inadequate drainage, and evapo-concentration in the soil profile.

Worldwide agricultural productivity losses of salt-inflicted soils have been estimated at $10 billion per year (Ghassemi et al., 1995).

The overall problem of salt accumulation and impacts on soil and crops, well as continually increasing global population growth, has driven the intensive study of salt transport in irrigated regions (Duncan et al., 2008; Foster et al., 2018; Schoups et al., 2005). However, comparatively little research has been conducted on salt fate and transport in dominantly non-irrigated desert catchments that are often upstream of productive agricultural catchments. Naturally occurring salt afflicted regions are less regulated than irrigated catchments due to the apparent distance from human activity and associated human intervention. However, headwater upland catchments have been recognized as sources of high sediment generation with steep gradients, high runoff volumes, thin vegetation cover, and active geomorphic processes (Stenson et al., 2011; Zimmer, 2021). Consequently, these upland catchments are also susceptible to high volumes of salt transport, and therefore understanding and regulation of upstream non-irrigated catchments could be a key factor in reducing the impact of salinity globally. For example, Biggs et al. (2013) found that small upland catchments have a greater export/import ratio of salt as compared to major downstream catchments using a mass balance approach from 55 gauging stations. Stenson et al. (2011) noted the importance of salinity exports in unregulated upland catchments to the increasing salinization of Australia's Murray-Darling Basin using the lumped-parameter 2CSalt salinity model. Zimmer (2021) used field measurements and mass balance approaches in a high-desert watershed in southeastern Colorado, USA, and found that salt loadings to the receiving Arkansas River are significant.

However, of these studies, none have systematically explored and quantified the impact of high-intensity storms on salt mobilization, movement, and in-stream loading within high-desert watersheds. The results of Zimmer (2021) suggest that high-intensity storms in semi-arid regions can have a large impact on salt transport in upland catchments. However, the findings were limited to years with stream data, and did not explore the mobilization and hydrologic pathways of salt loading to the stream network. With climate extremes predicted to increase in the future (Coumou & Rahmstorf, 2012; Francis et al., 1998), understanding the role of high-intensity storms in high-desert watersheds can be important in estimating salt loading to downstream irrigated regions.

Numerical computer models have been extensively used to simulate salt processes on a variety of spatial scales and could be used to investigate the impact of high-intensity storms on salt movement. For example, SWAT-Salt is the combination of the widely known Soil and Water Assessment Tool (SWAT) and a coupled salinity module (Bailey et al., 2019). SWAT (Arnold et al., 1998) is a process-based conceptual watershed-scale hydrologic model that was developed by the USDA Agricultural Research Service to evaluate best management practices for water supply and nonpoint source pollution in large river basins. SWAT has been popularized globally because the minimum requirements to run a simulation (i.e., a digital elevation model (DEM), land use/land cover map, and soil map) are often readily available through public government organizations. The SWAT website (http://swatmodel.tamu.edu) provides extensive model documentation, including theoretical documentation with equations, a user's manual defining model inputs and outputs, a developer's manual, and tutorial videos for the project setup in the ArcSWAT interface of an example watershed.

SWAT-Salt, the salinity module coupled to SWAT, was one of the first process-based models to consider salt transport within all major hydrologic pathways and salt chemical reactions (precipitation-dissolution, complexation, and cation exchange within the soil layers and the alluvial aquifer) for individual ions at the watershed scale (Bailey et al., 2019). SWAT-Salt focuses on the transport and effects of major salt ions. Since the SWAT hydrologic model is well-researched and the salinity module is well-detailed (i.e., division into the eight ions for all major hydrologic pathways), the SWAT-Salt model was chosen in this study to quantify a gap in research knowledge of salt transport and mobilization from largely undeveloped upland catchments. SWAT-Salt has been used to simulate salt ion transport in irrigated watersheds (Bailey et al., 2019; Hosseini and Bailey, 2022), but has not yet been applied to high-desert watersheds.

1.2 Summary of Objectives

The objective of this thesis is to quantify the impact of climate change and increasing storm intensity on the mobilization, movement, and loading of salt in an upland watershed in a semi-arid region. This is achieved by applying SWAT-Salt to the undeveloped Purgatoire River Watershed (8,922 km^2) in southeastern Colorado. We use a modeling approach so that loads can be estimated for years and conditions that do not have field data, and so that salt sources and transport pathways can be quantified. The model is calibrated and tested against stream discharge and in-stream salt ion loads for several gage sites within the watershed, and then used to quantify the impact of increasing future storm intensity. Results also provide insights into hydrologic pathways that govern in-stream salt loading and general spatial patterns of salt mobilization and transport to the Purgatoire River and its tributaries. As the Purgatoire River discharges to the Arkansas River, which services many irrigated areas in southeastern Colorado and western Kansas, this study also provides a sense of the salinity impact of high-desert watersheds on rivers that carry water downstream for irrigation use.

The remainder of this thesis is organized as follows: Section 2 presents the Methods, including a description of the study region and the construction and application of the SWAT-Salt model to the Purgatoire River Watershed for historical conditions and scenarios of increasing storm intensity; Section 3 presents the results of model calibration, testing, and scenario analysis; and Section 4 provides a summary of major findings and conclusions from the study results.

2. METHODS

2.1 Study Region: Purgatoire River Watershed

The Purgatoire River Watershed, with a drainage area of 8,935 km^2, is one of the largest contributing watersheds to the Arkansas River within the Upper Arkansas River basin (Figure 1), a subbasin of the Arkansas-Red-White basin. The headwaters of the Purgatoire River originate in the Sangre de Cristo Mountain range near Weston, CO. The Purgatoire flows ~194 mi from the mountains to the Arkansas River outlet near Las Animas, CO, in Bent County.

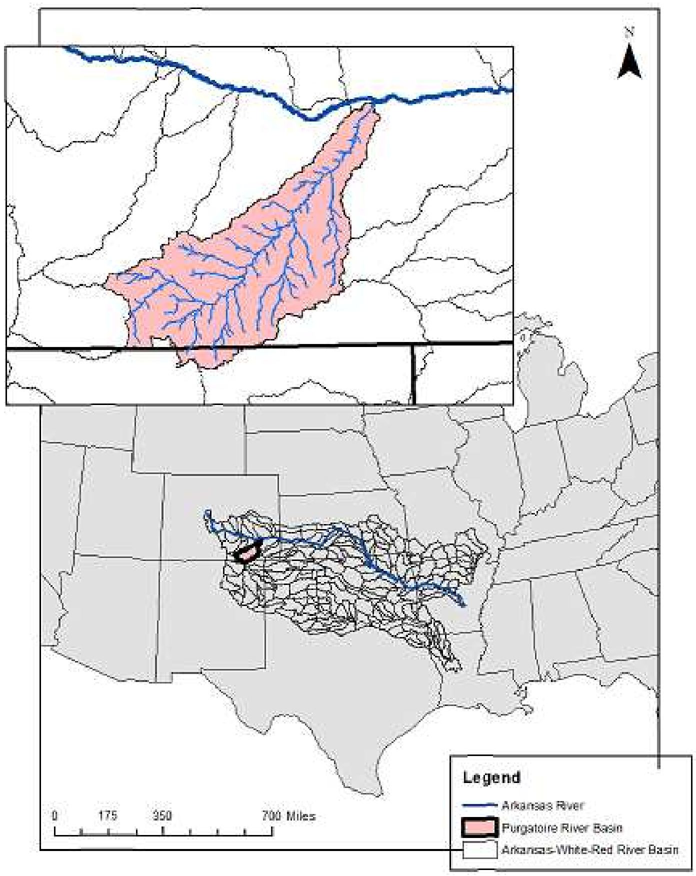

Figure 1- Map of the Purgatoire River watershed within the HUC8 delineated Arkansas-White-Red River Basin.

The western, mountainous region of the watershed is quite different than the eastern rangeland that meets the edge of the Great Plains, and the two regions are often delineated with the Interstate-25 corridor of Colorado. Discharge from the Purgatoire River travels through southeastern Colorado, Kansas, Oklahoma, and Arkansas before reaching the Mississippi River (Figure 1). Snowmelt is the main source of water for the Purgatoire River. Discharge in the eastern portion of the watershed is largely controlled by the dam at Trinidad Reservoir implemented by the U.S. Army Corps of Engineers for irrigation storage, flood control, and recreational activities. The dam releases are often paused outside of the irrigation season for storage, generally between mid-October and mid-April (Purgatoire Watershed Partnership, 2014). Consequently, the downstream section of the Purgatoire relies on inflow from tributaries during the winter season, most notably the Chacuaco River. Other tributaries of the Purgatoire are mainly ephemeral and have carved a complex network of canyons and mesas throughout the basin during intense rainfall events.

The west portion of the Purgatoire River Watershed (west of Trinidad) lies on top of the Central Raton Basin and the east portion lies on the Cheyenne-Dakota aquifer. The water table within the Cheyenne-Dakota aquifer is approximately 300 feet below the surface (Purgatoire Watershed Partnership, 2014). Some studies have evaluated groundwater supplies in the Raton Basin aquifer, but little research has been conducted regarding groundwater in the Cheyenne-Dakota aquifer and within the entire Purgatoire River Watershed.

The dominant land uses are herbaceous rangeland and mixed shrubland covering 53% and 23% of the basin, respectively (Figure 2A). The dominant vegetation in the shrubland is piñon-juniper woodlands. Less than 1.3% of the entire basin is designated as developed by the National Land Cover Database (NLCD). Evergreen and mixed forests cover most of the mountainous regions and are found sparsely scattered throughout the rangeland. 61.3% of the basin is privately owned, but the basin also encompasses the U.S. Army base Pinon Canyon Maneuvering site and National Grasslands and Forests (Purgatoire Watershed Partnership, 2014). The occupied land is dominated by an agrarian economy with ranging cattle, particularly in the main canyon.

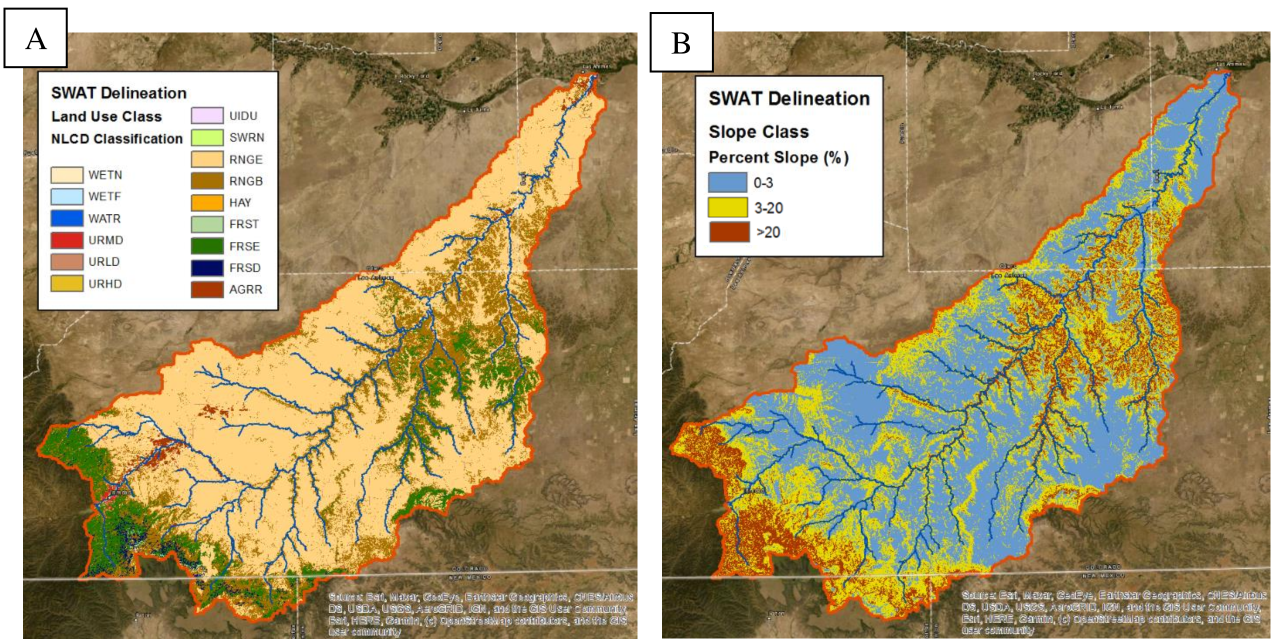

Figure 2- A) Land use delineation for the Purgatoire River Watershed (NLCD, 2011). B) SWAT Slope Class for the Purgatoire River Watershed. Both figures exclude the mountainous region of the basin.

A defining characteristic of this watershed is the steep slope gradients, with an average slope of 12% and maximum slope of 249% (Figure 2B). The elevation ranges from just under 4,267 m (14,000 ft) in the Sangre de Cristo Mountains to 1,188 m (3,900 ft) in the rangeland. High slope gradients are not only defining in the mountainous region, as many riparian areas of the Purgatoire River are lined with steep sloped plateaus throughout the rangeland (Figure 2B).

The Purgatoire River basin remains relatively mild for a semi-arid catchment, with precipitation during the summer months (June-August) extremely variable. Most rainfall occurs between April and October, with high-intensity storm events often occurring between July and September. These intense summer storms produce more runoff and streamflow than winter and spring precipitation (Purgatoire Watershed Partnership, 2014).

Since the region is largely undeveloped, weather stations are sparse throughout the basin. Trinidad, the largest city in the watershed, has a hub of weather stations, and there are several stations monitored by the Colorado Agriculture Meteorological Network (CoAgMet) that lie within or very close to the basin (Figure 3). The Hoehne Station (HNE01) is located within 10 miles of the Trinidad Airport and has historical climate data since the year 2000. The La Junta Station (LJT01), Las Animas Station (LMS02), and Rocky Ford Experimental Station (RFD01) are all outside the boundaries of the watershed, but close to the outlet (see Figure 3). These three stations have reported climate data since 1972, 2020, and 1992, respectively. Climate data from the Trinidad Airport, La Junta Station, and Rocky Ford Station were evaluated for this study and will be further discussed in the hydrologic modeling section.

A monthly climate summary from July 1st, 1898, to June 16th, 2016, recorded at TRINIDAD Station #058429 records an annual average maximum and minimum temperature of 86.8°F in July and 18.9°F in January. The average annual precipitation and snowfall recorded for this period were 396.2 mm and 1,290.3 mm, respectively. This estimate of average annual precipitation near Trinidad, CO, is higher than other gages in the basin and the three stations outside the basin, likely due to the extended period of record. The Hoehne Station in northeast Trinidad recorded an average annual precipitation of 254.0 mm between 2001-2020. Farther northeast near the outlet, the Rocky Ford and La Junta stations have recorded average annual precipitation values of 259.1 mm and 256.5 mm, respectively, since 1993 and 2006.

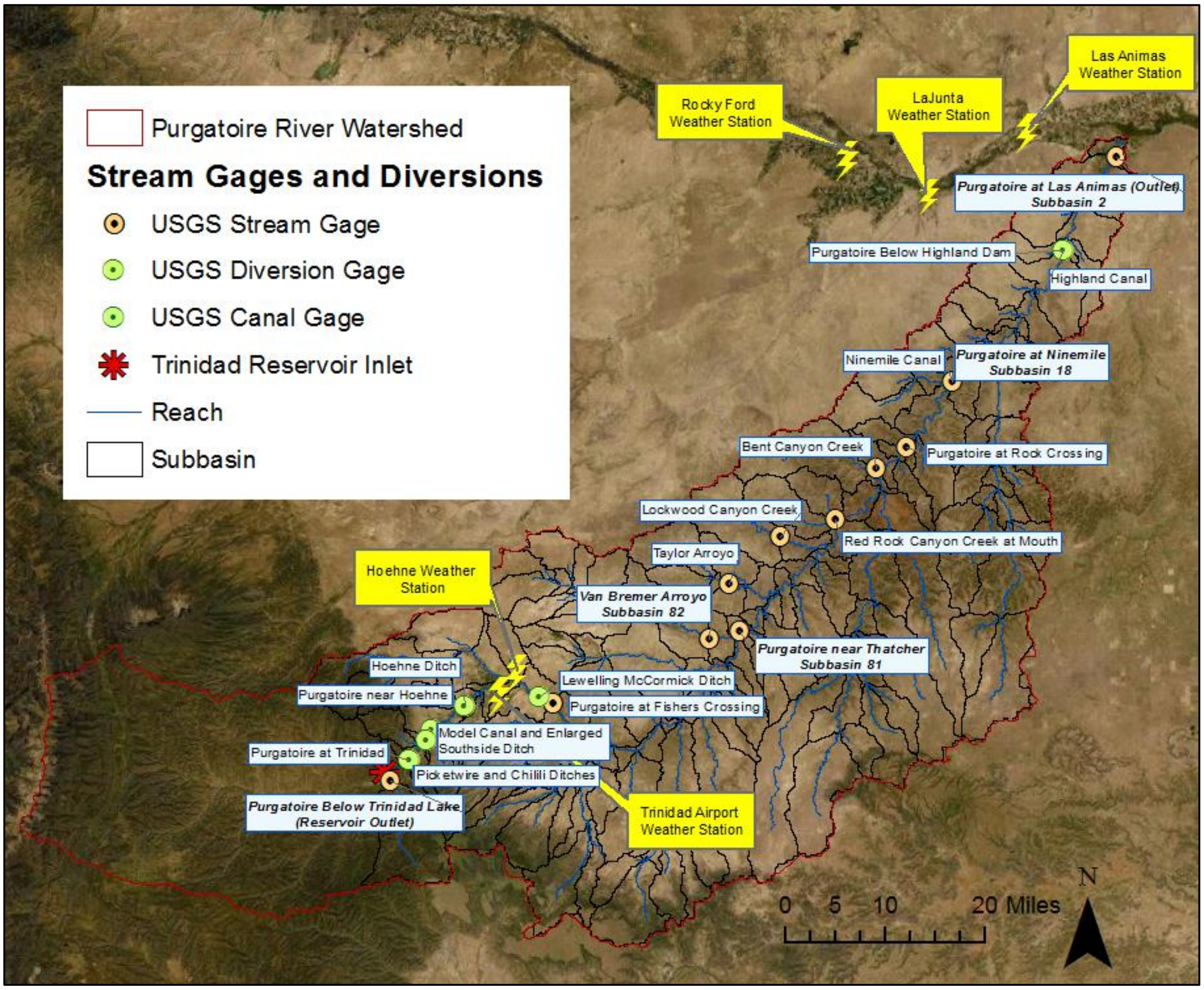

Figure 3- Map of each USGS stream gage, USGS diversion gage, CoAgMET weather stations, the Trinidad Reservoir inlet to the basin, and the delineated stream network of the Purgatoire River Watershed.

The Arkansas River Basin (see Figure 1) contains an abundance of productive agricultural regions. However, previous studies have demonstrated that excessive irrigation and inadequate drainage has led to salinized and waterlogged soils in many regions within Colorado (Gates et al., 2006). Although increased salinization is partially due to agricultural practices, salt loads in the basin could also originate in upland, high-desert watersheds such as the Purgatoire River Watershed. Zimmer (2021) reported that in 1990, the Purgatoire River exported approximately 64,600,000 kg of salt to the Arkansas River, which accounted for approximately 22% of the salt in the Arkansas River downstream of the confluence. The same analysis was conducted for 2020, and the Purgatoire River was noted to export approximately 18,040,000 kg of salt to the Arkansas River, which accounted for 11% after merging. Differences between the salt exports in 1990 and 2020 were due to differences in annual rainfall depth and the occurrence of summer thunderstorms. The total annual precipitation in 2020 was 47% less than in 1990. These results indicate that upstream desert catchments can have a large effect on downstream salinity loads in irrigated catchments, and that salinity loading could be highly correlated with annual precipitation.

Salt loads within the Purgatoire River Watershed and other high-desert, semi-arid watersheds can be impacted by long-term changes in precipitation and temperature. However, perhaps more important is the potential impact of high-intensity storms, which can mobilize and transport salt via erosion in steep-gradient regions, such as in the Purgatoire River Watershed (see Figure 2B). Very heavy precipitation events, defined as the heaviest 1% of all daily events from 1901 to 2012, and the length of dry spells are projected to increase across the United States (Georgakakos, A. et al., 2014). Whereas global climate models have not suggested a strong change in average annual precipitation throughout the 21st century in southeastern Colorado (Hegewisch & Abatzoglou), there likely will be an increase in storm intensity due to increases in the moisture holding capacity of the atmosphere and changing the storm generating mechanisms that drive extreme events (Colorado Water Conservation Board, 2019). Zimmer (2021) used mass balance equations based on field data within the Purgatoire River Watershed, concluding that high-intensity storms in semi-arid regions can have a large impact on salt transport from upland catchments. With this knowledge, this research attempts to quantify changes in salt loads with increasing storm intensity.

2.2 Quantifying Salt Loading Using SWAT-Salt

Numerical computer models have been extensively used to simulate salt processes on a variety of spatial scales. Many studies have utilized salinity models, such as the Soil-Water-Atmosphere-Plant model (SWAP) at the field-scale to better quantify the direct implications to specific crop growth and agriculture (Jiang et al., 2011). However, field-scale models often rely on vast amounts of high-resolution field data, which is not as feasible to obtain at the watershed-scale. Available models to simulate salt transport and mobilization at the watershed-scale include SWAT-Salt, SAHYSMOD, MT3DMS, UNSATCHEM coupled with HYDRUS, SWAT-SF, BC2C, 2CSALT, and more. Such models have been mainly utilized to quantify the impacts of salinization in agricultural watersheds (Burkhalter et al., 2006; Chang et al., 2021). However, both MT3DMS and SAHYSMOD lack salt reactive chemistry (Bailey et al., 2019), and the models that do include salt reactive chemistry have typically been utilized for smaller-scale field studies, such as UNSATCHEM coupled with HYDRUS (Hanson et al., 2008; Šimůnek et al., 2016). 2CSALT and the Biophysical Capacity to Change model (BC2C) were both developed specifically to produce a model that is easily transferrable to a large number of catchments with comparable results and lacks the level of detail needed for this study.

SWAT-Salt is the combination of the widely known Soil and Water Assessment Tool (SWAT) and a coupled salinity module (Bailey et al., 2019). SWAT-Salt is one of the first models to consider salt transport within all major hydrologic pathways and salt chemical reactions (precipitation-dissolution, complexation, and cation exchange within the soil layers and the alluvial aquifer) for individual ions at the watershed scale (Bailey et al., 2019). The eight major ions this model focuses on the transport and effects of are SO_4^{2-}, Cl^-, CO_3^{2-}, HCO_3^-, Ca^{2+}, Na^+, Mg^{2+}, and K^+. Since the SWAT hydrologic model is well-researched and the salinity module is well-detailed (i.e., division into the eight ions for all major hydrologic pathways), the SWAT-Salt model was chosen in this study to quantify a gap in research knowledge of salt transport and mobilization from largely undeveloped upland catchments. This rest of this section provides an overview of the SWAT model and its salinity module with application to the Purgatoire River Watershed.

2.2.1 Simulating Hydrologic Processes Using SWAT

SWAT Theory

SWAT (Soil and Water Assessment Tool, Arnold et al., 1998) is a process-based, semi-distributed river basin model that was developed by the USDA-ARS to simulate the movement of water, nutrients, and sediment in a watershed system. Within a SWAT hydrologic model, watersheds are divided into smaller subbasins that are more spatially homogenous to reference different areas of the basin. Subbasins are comprised of hydrologic response units (HRUs), which each represent a unique combination of land use, soil type, and slope. The HRU is the smallest computational unit used in SWAT to calculate surface runoff, shallow aquifer dynamics, erosion, soil water content, and nutrient cycling. These various pathways or fluxes of water, sediment, nutrients, etc., at the HRU level are then combined, and a weighted subbasin value is calculated.

Precipitation and irrigation drive the hydrologic processes in SWAT, with water balance, nutrient mass balance, and sediment mass balance performed for four main systems: the land surface system, the soil system, the aquifer system, and the stream network system. For example, the water balance in the soil profile is simulated using the following equation:

$$SW_t = SW_0 + \sum_{i=1}^{t} R_{day} - Q_{surf} - E_a - w_{seep} - Q_{gw} \qquad \textit{(Equation 1)}$$

where SW_t is the final soil water content (mm H_2O), SW_0 is the initial soil water content on day i, t is the time (days), R_{day} is the amount of precipitation on day i (mm H_2O), Q_{surf} is the amount of surface runoff on day i (mm H_2O), w_{seep} is the amount of water entering the vadose zone from the soil profile on day i (mm H_2O), and Q_{gw} is the amount of lateral return flow on day i (mm H_2O). SWAT represents base flow as return flow originating from groundwater. Percolating water is rationed to either a shallow or a deep aquifer system. The shallow aquifer is the source of return flow to the main channel in the water balance, and water can also be lost from the shallow aquifer through revap to the soil profile in dry conditions. The deep aquifer can contribute return flow to streams both within and outside of the watershed.

SWAT Model for the Purgatoire River Watershed

The SWAT model for the Purgatoire River Watershed is applied to the time period 1990-2020 due to availability of salt ion data. Required datasets for delineation and creation of subbasin boundaries, the stream network, and hydrologic response units (HRUs) include a digital elevation model (DEM) (30-m) and land cover distribution raster (30-m) from the National Resources Conservation Service (NRCS) Geospatial Data Gateway (https://datagateway.nrcs.usda.gov/GDGOrder.aspx). The DEM is a product of the National Elevation Dataset (NED), and the land cover distribution is a product of the National Land Cover Database (NLCD, 2011). The soil map of the Purgatoire is a SSURGO dataset, also downloaded from the NRCS. Within ArcSWAT, minimum subbasin delineation area was set to 2500 ha (~9.7 mi^2), to adequately depict the tributary network and save computational time, resulting in 169 subbasins. The subbasins were further divided into HRUs, based on unique combinations of land use, soil type, and slope. Using thresholds of 1% land use, 5% soil, and 0% slope resulted in 5,643 HRUs.

The Trinidad reservoir controls the downstream discharge throughout the eastern rangeland of the Purgatoire watershed. Since this study is focused on salt transport in semi-arid regions, the mountainous region of the Purgatoire watershed was not included in the SWAT model watershed delineation. The United States Geologic Survey (USGS) has recorded daily outflow from the Trinidad Reservoir through the entire simulation period. The daily reservoir outflow, obtained from the USGS gaging site Purgatoire River Below Trinidad Lake #07128500 (see Figure 3) was entered into the model as a source of inflow to the model domain. Excluding the upstream mountainous region of the watershed decreased the modeled F to 7,081km^2 from 8,935 km^2.

The final land use distribution within the modeled portion is 65.5% rangeland-grasses, 22.3% rangeland-brush, and 10.3% forest (dominantly evergreen), (see Figure 2A). Only 0.31% of the modeled portion is residential. Three slope classes were used within the HRU definition: 1) 0-3%, 2) 3-20%, and 3) >20% (see Figure 2B). The exclusion of the mountainous region resulted in 49.6%, 36.7%, and 13.8% of the area falling into the first, second, and third slope classes, respectively. Soils were a bit more evenly distributed throughout the modeled portion, with the most dominant soil series being Travessilla, covering ~19.7% of the watershed. Travessilla soils are hydrologic group (HSG) D soils and are mostly silty in texture. HSG C and D soils cover ~48% and ~43% of the modeled watershed, respectively.

Weather Data

SWAT requires daily precipitation and temperature data for the simulation period. The Parameter-elevation Relationships on Independent Slopes Model (PRISM, accessed at https://www.prism.oregonstate.edu/explorer/) was utilized to download daily precipitation and maximum/minimum temperature data (1988-2021) at a 4 km x 4 km scale at the centroid of each of the 169 subbasins. The daily maximum and minimum temperatures from PRISM corresponded well with the gage data in the region and were entered directly into the SWAT model. PRISM estimates of daily precipitation over-estimated values as compared to weather stations in the area for the period of interest but followed similar temporal patterns (Figure 4A). Initial runs of SWAT with the original PRISM precipitation data resulted in watershed outflow 3 times higher than reported at the outlet gage. Therefore, PRISM data was corrected based on daily data from the Hoehne weather station, using the relationship shown in Figure 4B

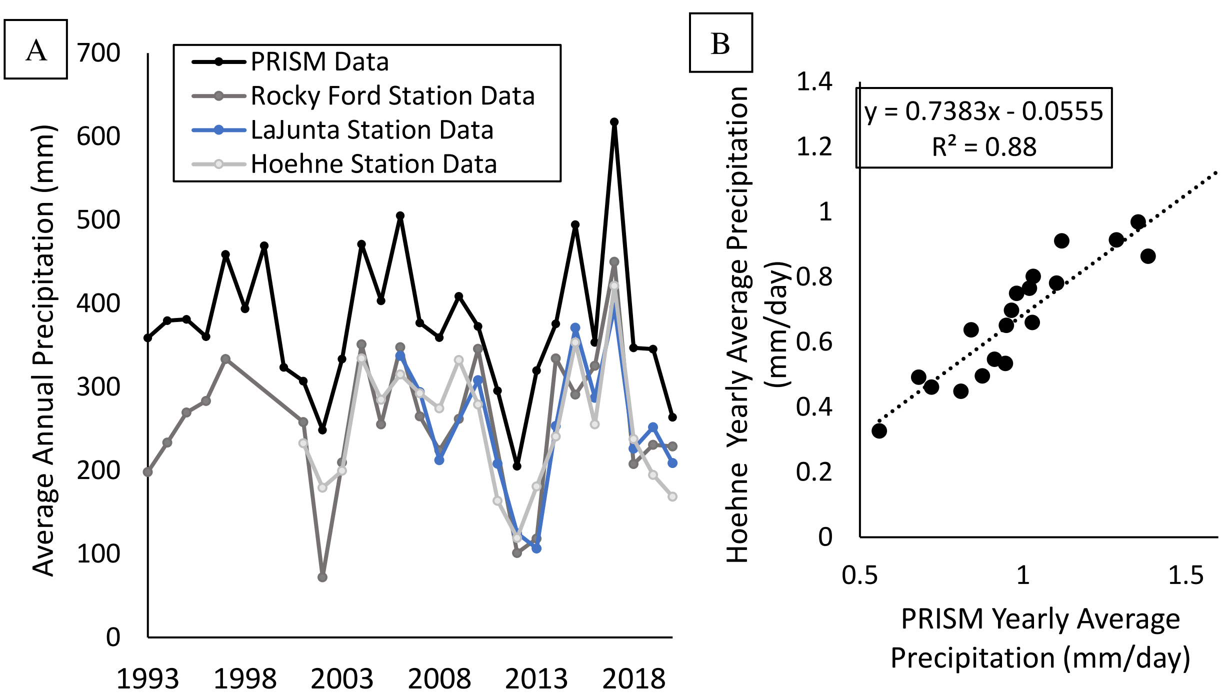

Figure 4- A) Yearly average annual precipitation from PRISM is consistently higher than the three CoAgMET stations near the Purgatoire Watershed. B) The regression equation shown between PRISM and the Hoehne Station yearly average precipitation values that was utilized to downscale PRISM daily values.

(R^2=0.88). This method allowed the spatial and temporal heterogeneity of PRISM data to be preserved.

We accounted for outflows along the Purgatoire River within the SWAT model. These consisted of canals and ditches that divert water from the Purgatoire River main stem for irrigation (see Figure 3). Eight canals monitored by the Colorado Division of Water Resources (DWR) were included in the SWAT model as diversions (Table 1). This allowed the subbasin mass balance of water to subtract the diverted canal water from the subbasin total stream flow. When more than one canal resided in the same subbasin, the canal diversions were summed for subtraction from the total flow. Two additional ditches resided within the Purgatoire watershed but were downstream of the Model Canal and not included in the model.

Table 1- Canal and stream diversions located along the Purgatoire River monitored by the Colorado Division of Water Resources (DWR).

Gage Name	DWR Abbreviation	Reporting Start Date	Reporting End Date	Subbasin number
Highland Canal	HILCANCO	1/15/2000	Present	8
Ninemile Canal at Ninemile Dam near Higbee	NMCHIGCO	10/1/1979	Present	18
Lewelling-McCormick Ditch	LMCDITCO	12/2/2018	Present	117
Hoehne Ditch	HOEDITCO	11/1/2007	Present	128
Model Canal	MODCANCO	10/30/2007	Present	128
Enlarged Southside Ditch	SOUDITCO	10/30/2007	Present	133
Chilili Ditch	CILDITCO	10/30/2007	Present	137
Picketwire Ditch	PIKDITCO	11/1/2007	Present	137

Fourteen USGS and DWR streamflow gages are included in the model as subbasin outlets. Five of these gages are located on tributaries or arroyos, and the remaining 9 gages are along the Purgatoire main branch (see Figure 3). The gage below Trinidad Reservoir was modeled as the inlet to the SWAT model domain. Additional gages that lie within the Purgatoire River Watershed were not utilized due to scarce or no streamflow data during the model period of 1990-2020. The additional gage names and the records of data availability are shown in appendix A (Table 9).

Model Calibration and Testing

Monthly river discharges measured at the Purgatoire River Watershed outlet were used for calibration and validation processes. The entire model duration was from January 1988-February 2021 with a two-year warm up period. The period from 1995-2005 was used to calibrate model parameters. The calibration results were subsequently validated during the period January of 2010 to February of 2021, and both calibration and validation periods included dry and wet years.

Mixed automatic and manual calibration practices were utilized for the estimating of hydrologic model parameters. Automatic calibration was conducted using SWAT-CUP (Abbaspour, 2012), and the goodness of fit between the modeled and measured runoff was evaluated using the coefficient of determination (R^2) and the Nash-Sutcliffe efficiency coefficient (NSE). Manual calibration was conducted by compared basin-wide hydrologic fluxes (evaporation, percolation, surface runoff, groundwater return flow, soil lateral flow) to annual estimates published for the continental United Stated between 2000-2013 (Reitz et al., 2017). This comparison allowed for the calibrated parameters, such as the curve number and main channel alluvium hydraulic conductivity, to better reflect realistic hydrologic conditions in southeastern Colorado.

The subbasins were divided into two categories for calibration: riparian zones and rangelands. Riparian zone subbasins encompassed the main stems of the Purgatoire and Chacuaco Rivers, and rangeland subbasins were designated as upland regions off the main stem.

This division was deemed valuable because the riparian zones show increased groundwater connectivity and vegetation density.

Five snow parameters were calibrated for the entire watershed. These parameters were the snowfall temperature (SFTMP, °C), snow melt base temperature (SMTMP, °C), melt factor for snow on June 21 (SMFMX, mm H_2O/°C-day), melt factor for snow on December 21 (SMFMN mm H_2O/°C-day), and the snowpack temperature lag factor (TIMP). An additional parameter, the maximum canopy storage (CANMX, mm H_2O), was calibrated by land use type. The remaining parameters were calibrated for both the riparian zone and rangeland subbasins (Table 2, column 1).

Table 2- Hydrologic calibration parameters and the bounds for the initial values.

Model Abbreviation	*Lower Bound*	*Upper Bound*	*Change*	*Final Value*
Riparian Zone Subbasins				
CN2.mgt	-30.00	0.00%	-4.73%	
LAT_TTIME.hru	0.00	8.81		3.22
HRU_SLP.hru	-14.81%	-4.93%	-9.48%	
SOL_K.sol	0.00	+15%	+9.05%	
CH_K2.rte	0.01	5.00		1.00
CH_N2.rte	0.03	0.05		0.041
GWQMN.gw	-1000	+1000	+106.20	606.20
REVAPMN.gw	-750	+750	-171.13	578.87
RCHRG_DP.gw	-0.05	+0.01	-0.043	0.007
ALPHA_BF.gw	0.005	0.100		0.006
ALPHA_BF_D.gw	0.00	1.00		0.36
GW_REVAP.gw	0.02	0.20		0.131
GW_DELAY.gw	-30	+90	-25.32	5.66
Rangeland Subbasins				
CN2.mgt	-30%	+10%	+7.83%	
LAT_TTIME.hru	5.46	14.00		10.56
HRU_SLP.hru	-9.35%	+1.97%	-4.00%	
SLSOIL.hru	0.00	+30%	+4.17%	
SOL_K.sol	0.00	+15%	+4.04%	
CH_K2.rte	0.00	0.65		0.00
CN_N2.rte	0.03	0.05		0.034
GWQMN.gw	-1000	+1000	-53.92	446.08
REVAPMN.gw	-750	+750	-234.15	515.85
RCHRG_DP.gw	+/-0.00	+0.05	+0.026	0.026
ALPHA_BF.gw	0.005	0.100		0.009
ALPHA_BF_D.gw	0.00	1.00		0.45
GW_REVAP.gw	0.02	0.2		0.026
GW_DELAY.gw	-30	+90	+43.24	74.24
Basin-wide				
CANMX.hru (RNGB, FRSE, FRST, FRSD)	0.00	10.00		6.44
CANMX.hru (RNGE)	0.00	5.00		3.20
EPCO.hru	0.50	1.0		0.892
ESCO.hru	0.75	0.95		0.873
SFTMP.bsn	-2.81	0.40		-2.24
SMTMP.bsn	0.53	2.18		1.09
SMFMX.bsn	2.64	3.91		3.15
SMFMN.bsn	1.11	3.32		1.27
TIMP.bsn	-0.25	0.58		-0.08

Automatic calibration was performed over the period 1995-2005 at the outlet of the Purgatoire River Watershed, USGS Gage #0712500, using SWAT-CUP. Parameters related to evaporation, groundwater exchange, and lateral flow (shallow groundwater flow) had the greatest impact on the model, as these forces drive the hydrologic cycle in the region. Specifically, the curve number (CN), effective hydraulic conductivity in main channel alluvium (CH_K(2), mm/hr), slope length for lateral subsurface flow (SLSOIL, m), and average slope steepness (HRU_SLP, m/m) had strong influences on lateral flow and surface runoff. Other parameters that demonstrated influence were the baseflow alpha factor (ALPHA_BF, 1/days), threshold depth of water in the shallow aquifer for "revap" or percolation to the deep aquifer to occur (REVAPMN, mm H_2O), and threshold depth of water in the shallow aquifer required for return flow to occur (GWQMN, mm H_2O).

2.2.2 Simulating Salt Ion Transport Using SWAT-Salt

Salinity Module for SWAT

The salinity module is implemented directly in the SWAT modelling code (FORTRAN language). Salinity fluxes are simulated through surface runoff, streamflow, groundwater flow, soil percolation, soil lateral flow, and groundwater upflux or "revap" to the soil profile. First, the mass balance of each salt ion is performed daily along with the water and nutrient calculations (phosphorus, nitrogen, etc) for each HRU soil layer and HRU aquifer unit within a subbasin. The HRU soil layer equation includes fluxes from surface water, groundwater, chemical dissolution and precipitation of salt minerals, soil lateral flow, percolation to the shallow aquifer, revap from the shallow aquifer, and irrigation (not relevant in this study). The HRU aquifer equation includes fluxes from groundwater flow, percolation, revap, precipitation, and dissolution (Bailey et al., 2019).

The changes in salt ion mass changes associated with precipitation and dissolution are calculated via mass balance and mass action equations. Precipitation is simulated if the ion content in the soil or aquifer layers is super-saturated, and dissolution is simulated if the mineral content in the soil layer or aquifer is under-saturated, based on the solubility of each mineral. Minerals included in the module are CaSO4, CaCO3, $MgCO_3$, NaCl, and $MgSO_4$. New concentrations based on the precipitation and dissolution equations are calculated on a daily time step for each soil layer and each aquifer of each HRU.

After the daily HRU mass balance and stoichiometric calculations, salt ions, water, sediment, and nutrients are transported to the main stem of each subbasin via surface runoff, soil lateral flow, and groundwater return flow. The salt ion load in each stream is then routed to the outlet of the subbasin, and the subbasin streams are routed through the stream network using SWAT's algorithms. The SWAT-Salt module is available for free to download at https://github.com/rtbailey8/SWAT_Salinity.

Modification to Include Salt Loads in Rainfall-Erosion Runoff

The equation implemented to estimate salt concentration in soil erosion was experimentally derived from hundreds of field samples taken from rainfall-runoff field experiments in the desert shrublands of the Upper Colorado River Basin, a similar semi-arid landscape (Cadaret et al., 2016). This is the first study that incorporates this equation into the SWAT-Salt routine. The polynomial simulates the concentration (mg/L) of total dissolved solids (TDS) in erosion runoff water:

$$\begin{aligned} TDS = {} & 160256 - 1.246x_1 + 0.0901x_2^2 - 0.00031x_2^3 + 1.296x_3 \\ & - 17.44x_4 + 0.1557x_4^2 + 1.287x_5 - 60865x_6 + 7659x_6^2 \\ & - 319x_6^3 + 171x_7 - 14.03x_7^2 \end{aligned} \qquad \textit{(Equation 2)}$$

where TDS is in mg/L, x_1 = runoff during a rain event (mm); x_2 = sediment concentration (g/L); x_3 = rock fraction of the soil; x_4 = sodium adsorption ratio (SAR); x_5 = cation exchange capacity (CEC) (mg/L); x_6 = pH of the soil water; and x_7 = electrical conductivity (EC) of the soil water. SWAT simulates runoff (mm) and sediment concentration (g/L) during a rainfall event. SAR and CEC equations are calculated based on the ion concentrations in the topsoil layer in the watershed. Once the TDS is calculated for each rainfall-runoff event, the individual ion concentrations are calculated from the ratio of each salt ion to TDS in the soil water of the top soil layer. Again, the salt mass associated with erosion rainfall-runoff events is transported to the subbasin main stem and routed through the watershed.

SWAT-Salt Model for the Purgatoire River Watershed

The SWAT model presented in Section 2.2.1 includes the salinity module with the use of additional salt input data. The salinity module requires initial concentrations of each of the 8 salt ions, SO_4^{2-}, Cl^-, CO_3^{2-}, HCO_3^-, Ca^{2+}, Na^+, Mg^{2+}, and K^+, in the soil and groundwater, initial salt mineral content in the soil and aquifer (%). Initial salt mineral data in the soil profile and the aquifer is required for $CaSO_4$ (gypsum), $CaCO_3$, $MgCO_3$, NaCl, and $MgSO_4$. NRCS SSURGO soil data was used to obtain salt mineral content for gypsum and calcium carbonate in the c horizon of the soil. The SSURGO soil map was spatially intersected with the 169 delineated subbasins. The weighted average of $CaCO_3$ and $CaSO_4$ for each subbasin was calculated based on the area of each soil map unit polygon (mupolygon), the mineral percent by weight in each mupolygon, and the total subbasin area. Each subbasin had unique initial values of average $CaCO_3$ and $CaSO_4$ (%) content (Figure 5). The south and eastern portions of the subbasin appear to have higher soil mineral content.

Since SWAT-Salt requires input values of mineral percent by weight at the HRU scale, we assumed each HRU within the same subbasin received the same initial mineral content. For example, subbasin 1 is comprised of HRUs #1-54, so HRUs #1-54 all began with initial $CaCO_3$ and $CaSO_4$ contents of 4.53% and 1.66%, respectively. HRUs #55-97 resided within subbasin 2 and began with initial $CaCO_3$ and $CaSO_4$ contents of 5.57% and 0.33%, respectively. We also assumed that the initial soil mineral content was equal to the initial aquifer mineral content due to a lack of data available from the aquifer and because the shallow aquifer seems to dominate the groundwater hydrology.

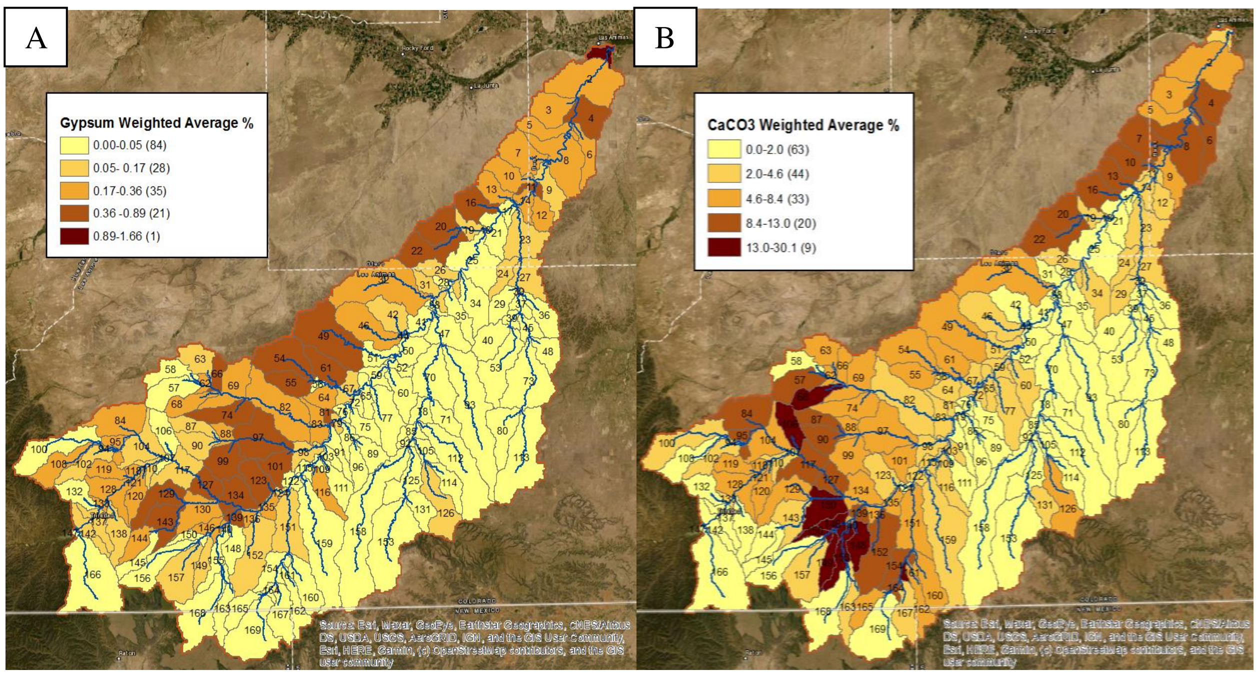

Figure 5- Spatial maps of subbasin weighted average values of CaSO4 (gypsum), (A) and CaCO3 (B) mineral content (% basis) in the soil profile. Data acquired from SSURGO.

Initial concentrations (mg/L) of each of the 8 salt ions in the soil and groundwater were estimated using the scarce samples recorded from USGS groundwater monitoring wells. There are 24 wells that have reported concentrations for the 8 salt ions modeled, and only 2 of the wells reported ion concentrations on two different dates. The earliest sample was taken in 1964, and the latest sample was taken in 1988. Table 3 shows the number of samples taken for each ion, the average concentrations from the samples, and the standard deviation of the concentrations. The full list of sample concentrations of each of the salt ions and USGS site numbers is provided in appendix B (Table 10).

Table 3- Historic USGS well water quality samples within the Purgatoire River basin for the salt ions modeled in this study.

	Ion Concentration (mg/L)							
	Ca^{2+}	Mg^{2+}	Na^{+}	K^{+}	Cl^{-}	SO_4^{2-}	HCO_3^{-}	CO_3^{2-}
Number of Samples	21	20	25	22	25	25	4	4
Average Conc. (mg/L)	222	122	333	5.4	110	1171	281	0
St. Dev	133.9	124.5	227.9	8.5	144.1	1030.9	124.4	0

A loose relationship to the SSURGO soil mineral data was utilized to spatially adjust the initial groundwater and soil concentrations for each of the salt ions. The average $CaCO_3$ mineral content in each subbasin from SSURGO was divided by the watershed average $CaCO_3$ mineral content. This ratio was calculated for each subbasin and multiplied by the average concentrations shown in Table 3 from the groundwater wells. $CaCO_3$ was used to derive the subbasin ratios because there is a greater range in percent $CaCO_3$ content throughout the watershed, as compared to $CaSO_4$. For example, subbasin 1 has an average $CaCO_3$ content of 4.54%, and the entire watershed has an average $CaCO_3$ content of 4.74%. The ratio multiplier developed for subbasin 1 is consequently 0.96. Each of 8 ion average concentrations displayed in Table 3 were multiplied by 0.96 to obtain the initial soil and groundwater salt ion concentrations for subbasin 1.

Because the streamflow from the Trinidad reservoir outlet is modeled as the watershed inflow, ion mass loading in the Purgatoire River from the reservoir outlet had to be included within the model. However, the site at the reservoir outlet has not reported any historical water quality samples of the 8 salt ions. The nearest USGS monitoring location that has recorded surface water quality samples of the 8 salt ions Purgatoire River at Madrid, CO, gage

#07124200. This site is just upstream of Trinidad Lake and reported 11 samples of Ca^{2+}, Na^+, Mg^2, Cl^-, 9 samples of HCO_3, and 6 samples of $CO_3{}^2$ between 1978-1981.

Ion concentrations were related to specific conductance values (uS/cm) reported on the same day from the upstream site at Madrid. Linear equations were developed to estimate ion concentration given specific conductance data for 7 salt ions, and the correlation coefficients are shown in Table 4. The regression equations were used to estimate daily ion concentration downstream at Purgatoire River Below Trinidad Lake given daily specific conductance. All 6 of the CO_3 samples reported a concentration of 0 mg/L with varying specific conductance values, so the CO_3 in the inflow was set to 0 mg/L and no linear equation was used. The regression of the other 7 ions to specific conductance values is shown in appendix C (Figure 18).

Table 4- Number of surface water quality samples taken at the USGS site Purgatoire River at Madrid and the correlation coefficient between the salt ion concentrations and specific conductance values.

	Ca^2	Mg^2	Na^+	K^+	Cl^-	$SO_4{}^{2-}$	$HCO_3{}^-$
Number of Samples	11	11	11	11	11	11	9
Correlation Coeff. R^2 with Specific Conductance (uS/cm)	0.93	0.95	0.87	0.18	0.77	0.73	0.94

The monitoring site below the reservoir reports specific conductance values from 1/19/1977-9/9/2010, and the values are reported using two different methods: filtered and unfiltered in a laboratory. Values reported before the year 2000 are unfiltered, and values reported after 2000 are unfiltered in a laboratory. Daily conductance values are required to obtain daily salt ion concentrations, but there are large gaps in the specific conductance data below Trinidad Lake. Linear interpolation between reported daily specific conductance values was utilized to fill the gaps between sample dates (Figure 6). The interpolated values for daily specific conductance from 1988-2010 were entered into the regression equations to obtain daily salt ion concentrations for the SWAT-Salt model.

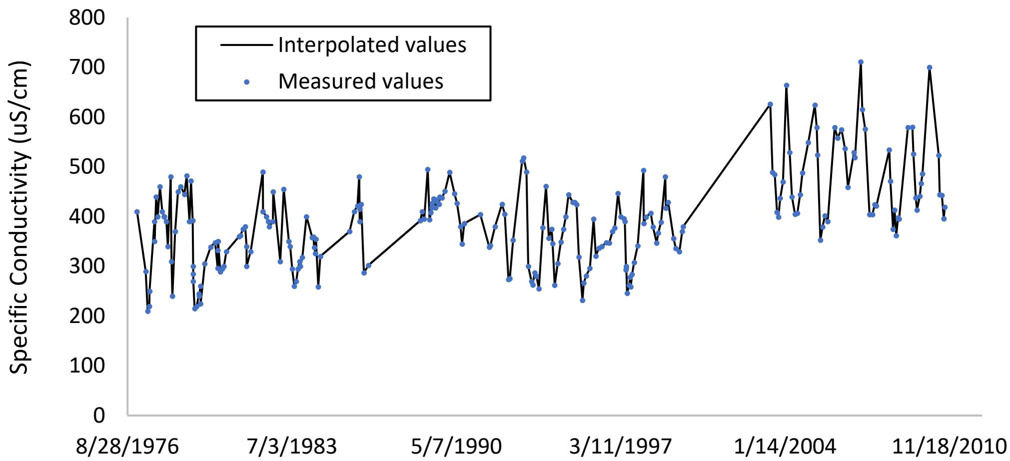

Figure 6- Measured and linearly interpolated daily specific conductance values at the site along the Purgatoire River below the dam used to calculate daily salt loads.

Model Calibration and Testing

SWAT-Salt results were compared to estimated monthly salt loads calculated using Load Estimator (LOADEST), a constituent load estimation Fortran program developed by the USGS. The executable and documentation can be downloaded from https://water.usgs.gov/software/loadest/. Any discharge data, specific conductance, and available salt ion concentrations from historic water quality samples from were supplied to LOADEST for the outlet gage, Purgatoire River at Las Animas. There were 58 samples of HCO_3^-, 68 samples of Ca^{2+} and Mg^{2+}, 74 samples of Cl^- and Na^+, 42 samples of K^+., and 89 samples of SO_4^{2-}. These samples were acquired over the period from 1961-2019.

Three different statistical estimation methods are considered in LOADEST, of which the adjusted maximum likelihood estimation (AMLE) is usually preferred. AMLE was used in this study, and the residuals of each ion load were determined to be normally distributed. Table 5 displays the AMLE regression statistics, the load bias in percent (BP), and the NSE for LOADEST results compared to measured values. Positive BP values indicate over estimation, and negative BP values indicate underestimation. The regression equation used to calculate the monthly load of each salt ion can be found in appendix D (Table 11).

Table 5- Satisfactory statistics from the LOADEST results for each of the 7 salt ions that had input data.

Salt Ion	**AMLE R^2 (%)**	**BP (%)**	**NSE**
HCO_3^{2-}	99.19	1.15	0.98
Ca^{2+}	97.42	-1.79	0.98
Mg^{2+}	94.98	2.79	0.96
Na^{+}	94.39	-0.05	0.94
Cl^{-}	89.71	-7.70	0.76
K^{+}	98.83	3.96	0.96
SO_4^{2-}	94.37	-1.55	0.95

The average monthly initial SWAT-Salt results were compared to the LOADEST results, and a few parameters required manual calibration. Salt calibration was conducted for the period 1990-2000, and validation was conducted for the period 2001-2010. The spatially heterogenous initial ion concentrations in both the groundwater and soil profile were manually calibrated for HCO_3^-, Na^+, and Mg^{2+}. Additionally, since no SSURGO data was available for the salt minerals $MgCO_3$, NaCl, and $MgSO_4$, all subbasins were given very small values of soil and aquifer mineral content (%). These values were manually adjusted during calibration.

In attempt to preserve the spatial heterogeneity of salt mineral content across the watershed, the assigned values of $MgCO_3$, $MgSO_4$, and NaCl soil and aquifer content (% basis) were related to the $CaCO_3$ content acquired with SSURGO data. Subbasins with $CaCO_3$ content greater than 15% received 0.1% of both $MgCO_3$ and $MgSO_4$, greater than 10% of $CaCO_3$ received 0.05% of $MgCO_3$ and $MgSO_4$, greater than 5% $CaCO_3$ received 0.02% of $MgCO_3$ and $MgSO_4$, and the remaining subbasins received 0.001% of $MgCO_3$ and $MgSO_4$. Subbasins with $CaCO_3$ content greater than 15% received 0.005% NaCl, greater than 10% of $CaCO_3$ received 0.001% of NaCl, greater than 4.5% $CaCO_3$ received 0.0005% NaCl, and the remaining subbasins received 0.0001% NaCl. The fractions of NaCl were lower than the mineral content of $MgCO_3$ and $MgSO_4$ because NaCl is more soluble. The mineral content differed for each subbasin but was assumed to be the same in the soil and the aquifer. SWAT-Salt results were compared to LOADEST results at the basin outlet, the Purgatoire River at Las Animas USGS Gage. The calibration period was 1990-2000, and the validation period was 2001-2010. The statistical indices, NSE and R^2 values, were calculated for monthly loads of each salt ion.

2.2.3 Quantifying the Impact of Climate Extremes on Salt Loading

In addition to using the SWAT-Salt model to investigate the mobilization, transport, and loading of salt ion mass from the landscape to streams under historical conditions, this study investigates and quantifies the impact of high-intensity storms on salt loadings. There is increasingly wide recognition that climate change is affecting the intensity of precipitation events. The Colorado Water Conservation Board (2019) stated that NOAA, the National Oceanic and Atmospheric Administration, has been developing new methods for constructing IDF, or intensity-duration-frequency, storm curves in the face of climate change using various global climate models. As part of this mission, the Colorado Water Conservation Board gathered data from the Climate Model Comparison Project, Phase 5 (CMIP5), for 1-degree grid cells to estimate model-driven changes in precipitation events between historical and future periods. The historical period used data from 1977-2006, and the future period projected data using two different approaches. One approach was using a 20-year window centered around 2050 (2035-2064), and the other approach was using a 30-year window centered around the year in which the climate model reached a warming threshold (1°C, 2°C, or 3°C). All cases used an ensemble of maximum and minimum precipitation values combined from approximately 20 global climate models.

The results demonstrated that extreme rainfall events in Colorado are projected to increase in intensity with each of the predicted future scenarios. For the 100-year daily rainfall event, the smallest median percent increase was ~5% from the 1°C warming threshold scenario, and the largest median percent increase was ~20% from the 3°C warming threshold scenario. The later scenario also demonstrated a maximum percent increase of ~35%. With these predictions in mind, this study evaluated 3 thresholds for increasing precipitation intensity in the Purgatoire River Basin: 0%, 5%, and 35% increases in daily precipitation of “extreme events.” The 3 scenarios are respectively referred to as Scenarios 0-2 throughout the rest of this paper. Scenario 0 acts as a baseline, scenario 1 demonstrates the median predicted intensity increase, and scenario 2 demonstrates the maximum predicted intensity increase.

To simplify the SWAT-Salt precipitation inputs, weather data from only 17 subbasins (~10% of the total subbasins) was used for the three scenarios. The 17 subbasins were chosen to represent the spatial heterogeneity of storms in the watershed (Figure 7). Since there were no 100-year storms during the model period, extreme events were defined as the top ~5% of storms in the 17 subbasins. This equated to 4 mm of precipitation in one day. The impact of increasing storm intensity was evaluated by increasing any daily precipitation event greater than or equal to 4 mm by the 3 thresholds through the entire model period. For example, if subbasin 2 received 10 mm of rain on 1/1/1988, the 3 different scenarios run in the model would consider 10 mm, 10.5mm, and 13.5 mm on that day.

The climate models evaluated predict the intensity of storms to increase in this region, but the average annual precipitation is not expected to increase. For this reason, the precipitation input data was normalized to maintain an average annual precipitation within 0.2 mm and 3.5 mm of the baseline scenario in scenarios 1 and 2, respectively. This normalization was achieved by subtracting depths of water for daily precipitation events less than 4 mm for each of the 17 subbasins. This resulted in averages of 0.15 mm and 1.70 mm of water subtracted from daily precipitation events for scenarios 1 and 2, respectively.

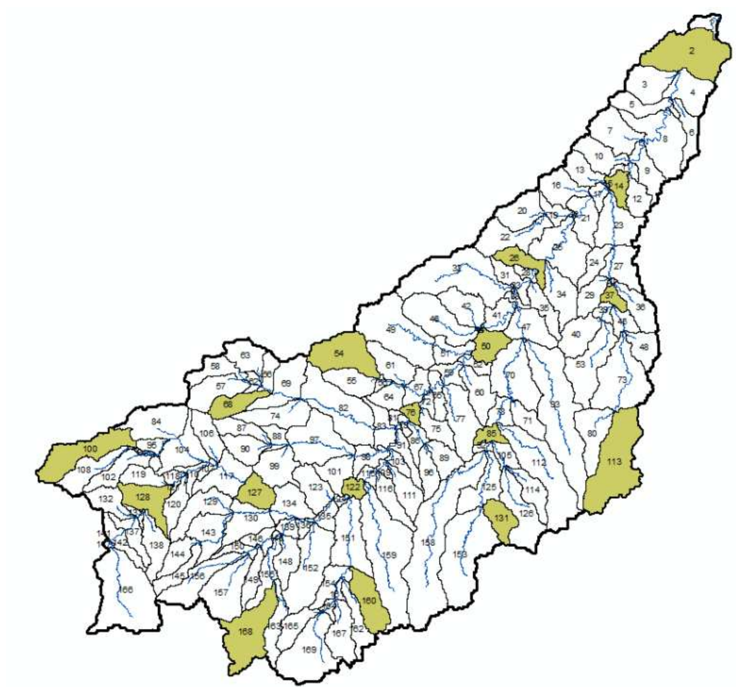

Figure 7- The 17 subbasins chosen highlighted in yellow green to demonstrate the spatial heterogeneity of precipitation inputs used within the SWAT- Salt future uncertainty scenarios.

3. RESULTS AND DISCUSSION

3.1 Hydrologic Processes

The final parameter results from the SWAT-CUP hydrologic calibration for the period 1995-2005 at the outlet of the Purgatoire River basin (USGS Gage #07128500) are shown in Table 2, column 4. Parameters that are different for each HRU, i.e., the curve number (CN2) report the percent change from initial HRU values (Table 2, column 3). Parameters that are the same for each HRU, i.e., lateral flow travel time (LAT_TTIME), report only the final value used. The outlet hydrograph accurately depicts the temporal changes in streamflow reported by USGS gage #07128500, such as the periods of drought that occurred in 2002-2003 and 2011-2012 and the wet years of 1999 and 2017 (Figure 8). The outflow typically mimics the temporal variation in the basin-wide average daily precipitation (mm/day).

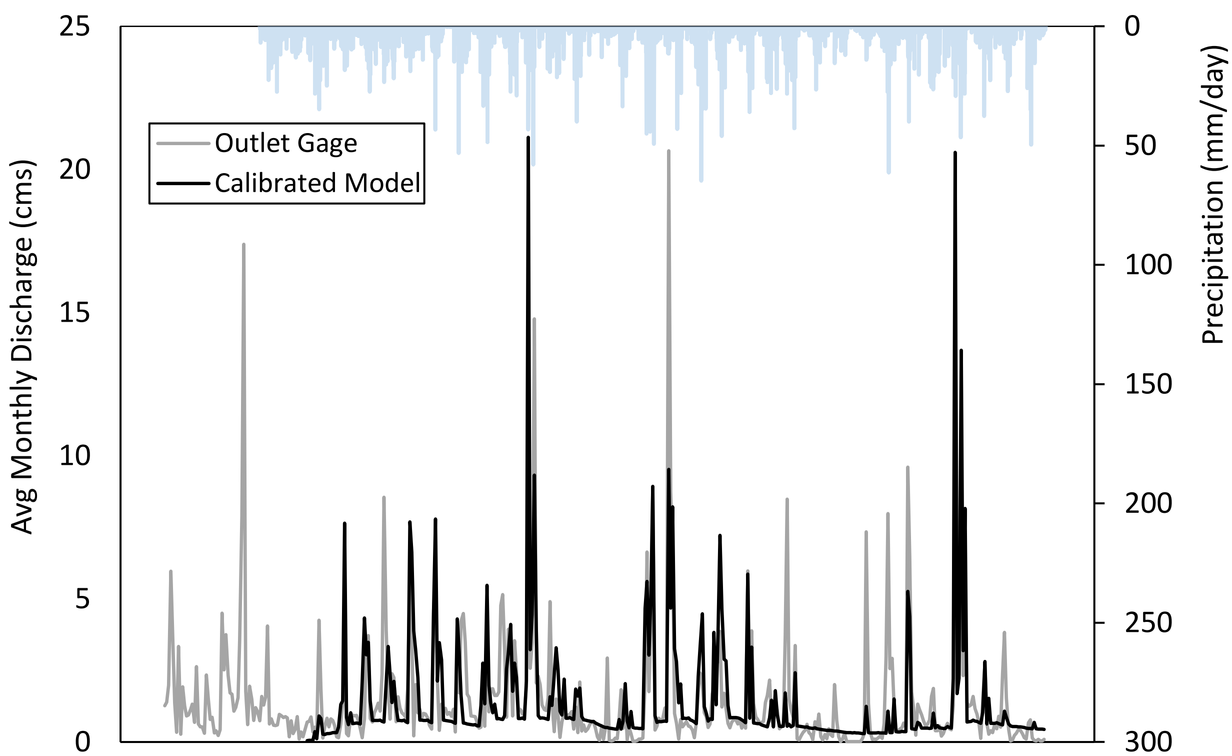

Figure 8- Hydrograph comparing satisfactory modeled results to USGS streamflow at the basin outlet, Purgatoire River at Las Animas, following the trends from the average watershed daily precipitation.

Although parameters were calibrated only for the outlet hydrograph, three other sites along the Purgatoire, Van Bremer Arroyo, Purgatoire River at Ninemile Dam near Higbee, and Purgatoire River at Thatcher, were included to further examine the calibration outputs. This provides a strong test to the model. Van Bremer Arroyo is a smaller (drainage area of ~450 km^2), intermittent tributary that releases just upstream of the Thatcher gage. The Thatcher gage is roughly 105 km upstream of the outlet and encompasses a drainage area of ~5,050 km^2 from the mountainous headwaters. The site at Ninemile Dam is roughly 45 km upstream from the outlet. These three sites were chosen to compare model results for additional data along the main stem, and the arroyo exemplifies how well the model captures intermittent streams.

The comparison between observed monthly gage discharge and simulated monthly streamflow at the outlet for the calibration period resulted in correlation statistics of NSE=0.62 and R^2=0.64 (Table 6). Based on the performance metrics of Moriasi et al. (2015), a NSE value greater than or equal to 0.50 and a R^2 value greater than or equal to 0.60 is satisfactory for monthly flow. The calculated total basin water yield from the monthly gage and modeled data are both 93.1 mm and 92.7 mm, respectively, for the calibration period (1995-2005). The validation period (January 2010-February 2021) demonstrated slightly weaker agreement (NSE=0.52 and R^2=0.60) but still displays satisfactory agreement. The basin's total water yield from the monthly gage and modeled data is 61.3 mm and 51.7 mm, respectively, for the validation period.

Figure 9 displays the calibrated model results at Thatcher, Van Bremer Arroyo, and Ninemile Dam. Note the differences in the discharge scale for each of these three sites. The results at Thatcher commonly underestimate baseflow, especially during the first 12 simulation years, because calibration was conducted to correctly estimate baseflow loads at the outlet.

Geologic maps of the Purgatoire River basin that report higher alluvium conductivity near the outlet support these results. The arroyo discharge is more difficult to model without precise precipitation data, however, the model does an adequate job with the intermittent stream.

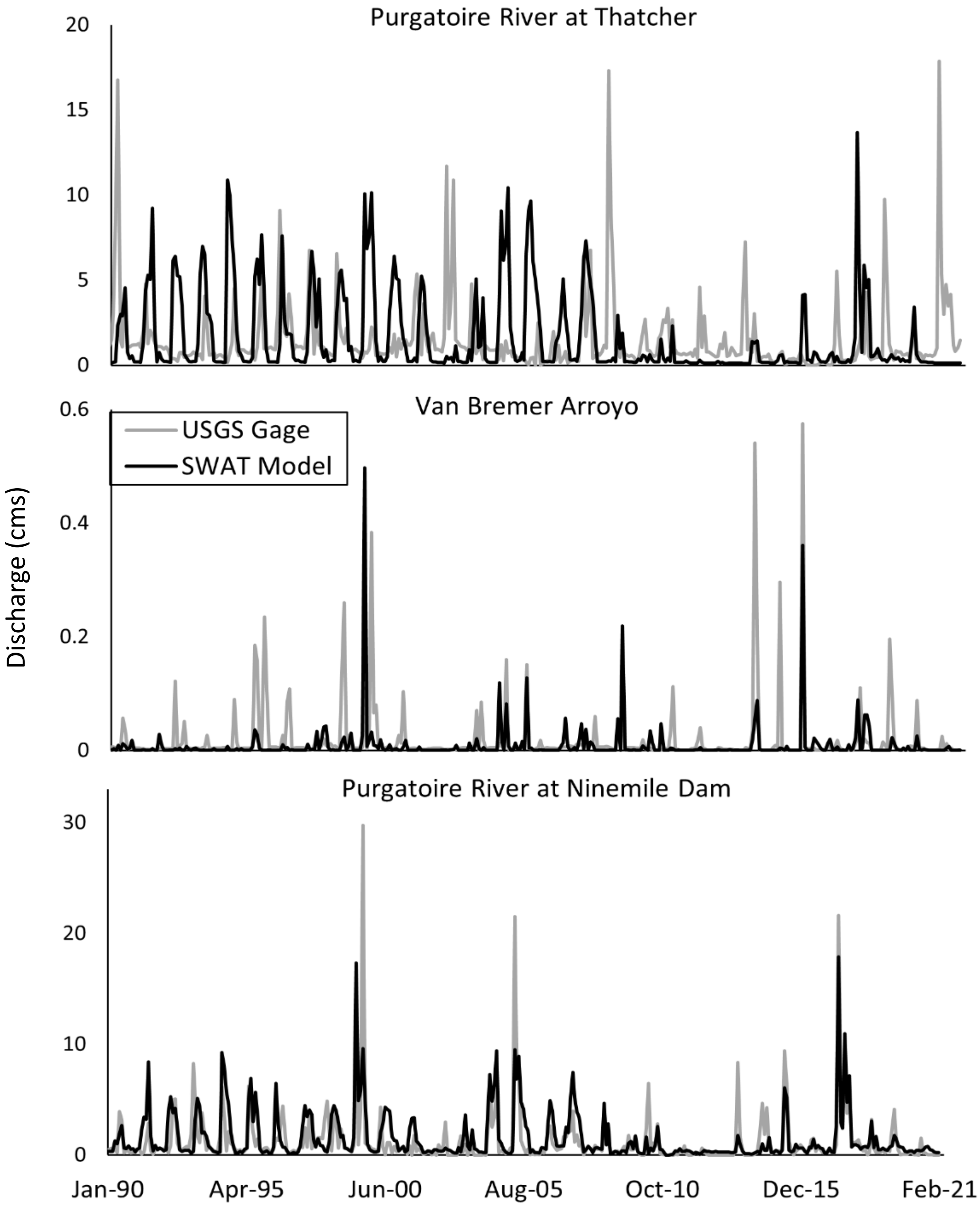

Figure 9- Hydrograph comparing satisfactory modeled results to USGS streamflow at three different sites: Purgatoire River at Thatcher, Van Bremer Arroyo, and Purgatoire River at Ninemile Dam.

Table 6 displays the statistical measures for the hydrologic model at the four sites. The validation results at the three sites along the mainstem are satisfactory, but the results at Van Bremer Arroyo are defined as poor (Moriasi et al., 2015).

Table 6- Statistical measures of performance for the hydrologic model compared to USGS streamflow data for the calibration and validation periods.

Site Name	*Calibration Period (1995-2005)*		*Validation Period (2010-Feb 2021)*	
	NSE	**R^2**	**NSE**	**R^2**
Las Animas (Outlet)	0.62	0.64	0.52	0.60
Thatcher	-0.07	0.35	0.70	0.77
Van Bremer Arroyo	-0.29	0.08	0.41	0.50
Ninemile Dam	0.48	0.48	0.77	0.78

Because soil profiles in the Purgatoire watershed are rarely at field capacity and there is a lack of vegetation in most of the basin, precipitation inputs tend to percolate into the soil as opposed to running off the ground surface. This phenomenon causes the majority of the hydrologic fluxes to the stream to be driven by soil lateral flow (Figure 10A). Hydrologic groundwater exchange and surface runoff are similar in contribution of water from the landscape to the Purgatoire River (Figure 10A).

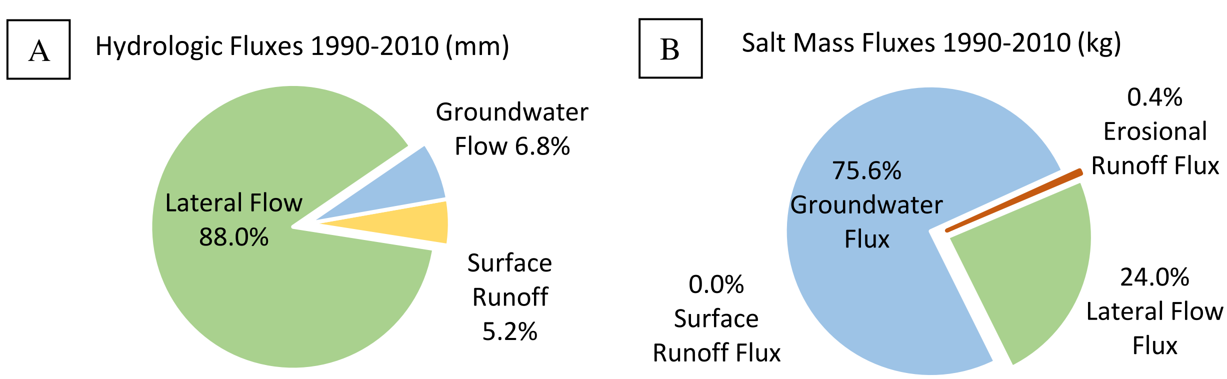

Figure 10- A) Hydrologic fluxes from the landscape to the Purgatoire River. B) Salt mass fluxes from the landscape to the Purgatoire River.

3.2 Salt Mobilization, Transport, and Loading Under Historical Conditions

Initial SWAT-Salt results suggested ion loads and ion concentrations followed similar temporal patterns as LOADEST results. However, modeled loads of HCO_3^-, Na^+, and Mg^{2+} were slightly smaller than the LOADEST results (although the same order of magnitude), so the initial concentrations of these three ions were manually calibrated. 0-30% increases in initial salt concentrations of HCO_3^-, Na^+, and Mg^{2+} in both the groundwater and soil profiles were evaluated in the SWAT-Salt model. The increases were the same in every HRU in both the groundwater and soil initial concentrations for each trial model run. The resulting initial salt concentrations were 30% greater for both HCO_3^- and Na^+, and 27% greater for Mg^{2+}.The statistical indices, NSE and R^2 values, were calculated for monthly loads of each salt ion (Table 8).

There were 20 months within the calibration period and 10 months within the validation period that LOADEST could not produce results for with the available water quality inputs. The yearly salt load correlation, R^2, between the 10 years that have complete LOADEST data, and the modeled results was determined to be 0.67. CO_3 was disregarded in this study, as all historic water quality samples have measured concentrations of 0 mg/L in the Purgatoire River. Similarly, K^+ was often disregarded because historic water quality samples have measured extremely small concentrations (< 1 mg/L), and this ion is largely insignificant compared to the remaining 6 salt ions.

Yearly average total modeled salt export from 1990-2010 at the outlet was ~64 million kg/year. SO_4^{2-}, Ca^{2+}, and HCO_3^- accounted for ~56%, ~20%, and ~14%, of the total salt exported from the Purgatoire River watershed, respectively. Together, these three ions make up 90% of the salt exported from the Purgatoire River basin. The statistical measures for these three ions are not categorized as good (Table 8), however, they are deemed satisfactory for this research to provide estimates of salt loads with very little measured input data. Figure 11 displays the full time series of modeled ion loads for SO_4^{2-}, Ca^{2+}, and HCO_3 compared to LOADEST results with the standard error of prediction. Mg+ and Na^+ both account for ~4.6% of the total salt exports. These five ions make up ~99% of the salt exported from the Purgatoire River watershed, with negligible loads of K^+ and CO_3^{2-}.

Table 7- Statistical measures of performance for the SWAT-Salt model compared to LOADEST results for the calibration and validation periods. Each ion besides Na and Cl performs satisfactory during the calibration period.

Salt Ions (avg monthly loads, kg/day)	*Calibration Period (1990-2000)*		*Validation Period (2001-2010)*	
	NSE	**R^2**	**NSE**	**R^2**
SO_4^2	0.11	0.25	-0.70	0.03
Ca^{2+}	0.14	0.32	-2.03	0.03
Mg^{2+}	0.14	0.30	-1.03	0.01
Na^+	-0.41	0.07	-0.81	0.01
Cl-	-0.64	0.34	-0.78	0.03
HCO_3^-	0.29	0.40	-0.13	0.22

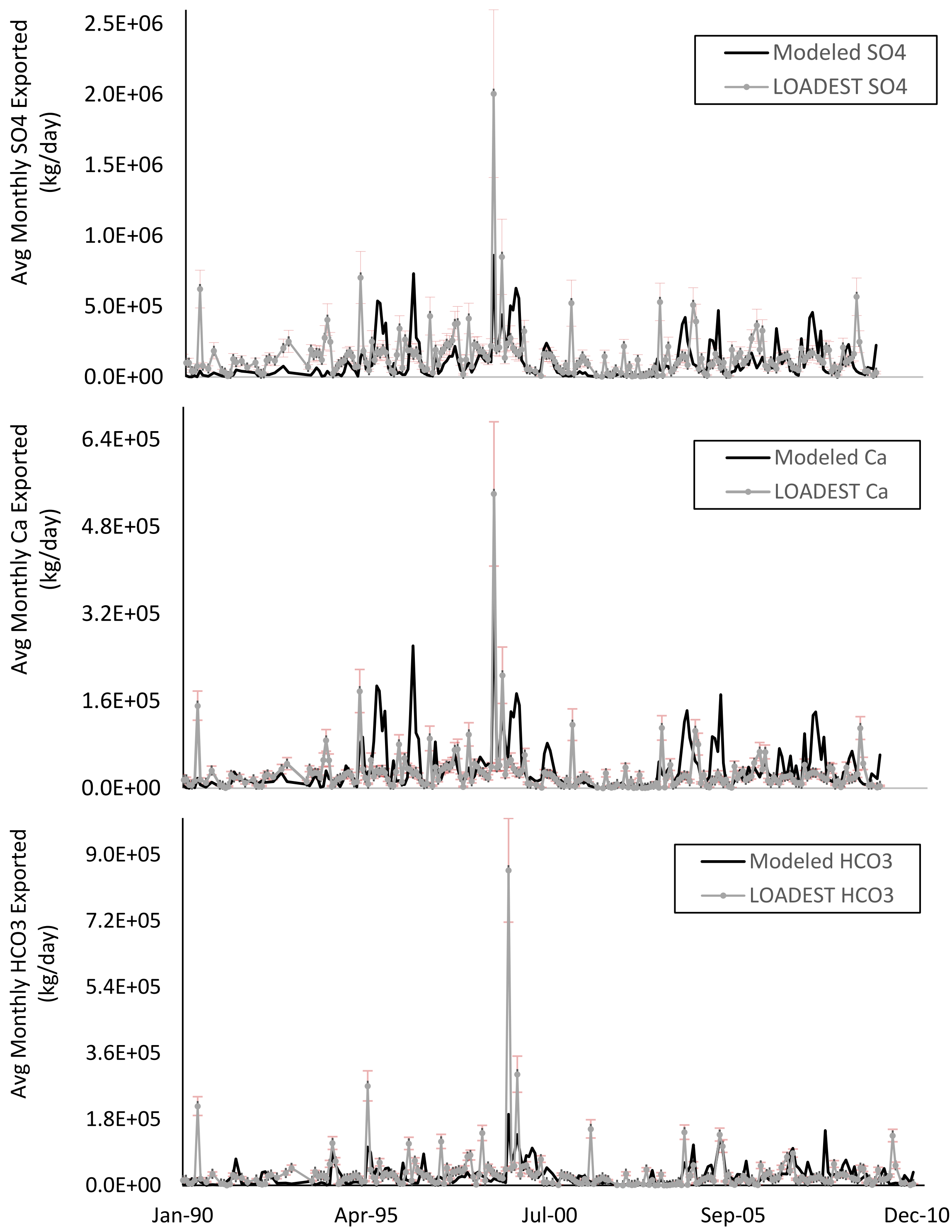

Figure 11- Average monthly modeled salt loads compared to LOADEST results (kg/day) for the three dominant salt ions in the Purgatoire Watershed. The SWAT-Salt model accurately captures the temporal variations in loads at the outlet.

75% of the total salt fluxes are from groundwater flow, and 24% of the total salt fluxes are from lateral flow, which SWAT often models as shallow groundwater flow. Combined, approximately 99% of the salt into the Purgatoire River is sourced from groundwater or shallow groundwater flow (see Figure 10B). The salt flux ratios do not mirror the hydrologic flux ratios, as lateral flow is the driver of hydrology. From these results, we observe that groundwater has higher concentrations of salt than the water in the soil profile, and most of the water in the soil profile leaches to the stream or groundwater. The retention time of water in the soil profile of semi-arid regions is short. Groundwater salt fluxes are more constant throughout the model period than the quick lateral flow pulses of salt that occur during larger precipitation events (Figure 12). There is a small, consistent amount of salt exported to the Purgatoire through erosional runoff, and these fluxes also show sharp increases during intense storm events (Figure 12). Little-to-no salt is exported to the Purgatoire River from surface runoff (see Figure 10B).

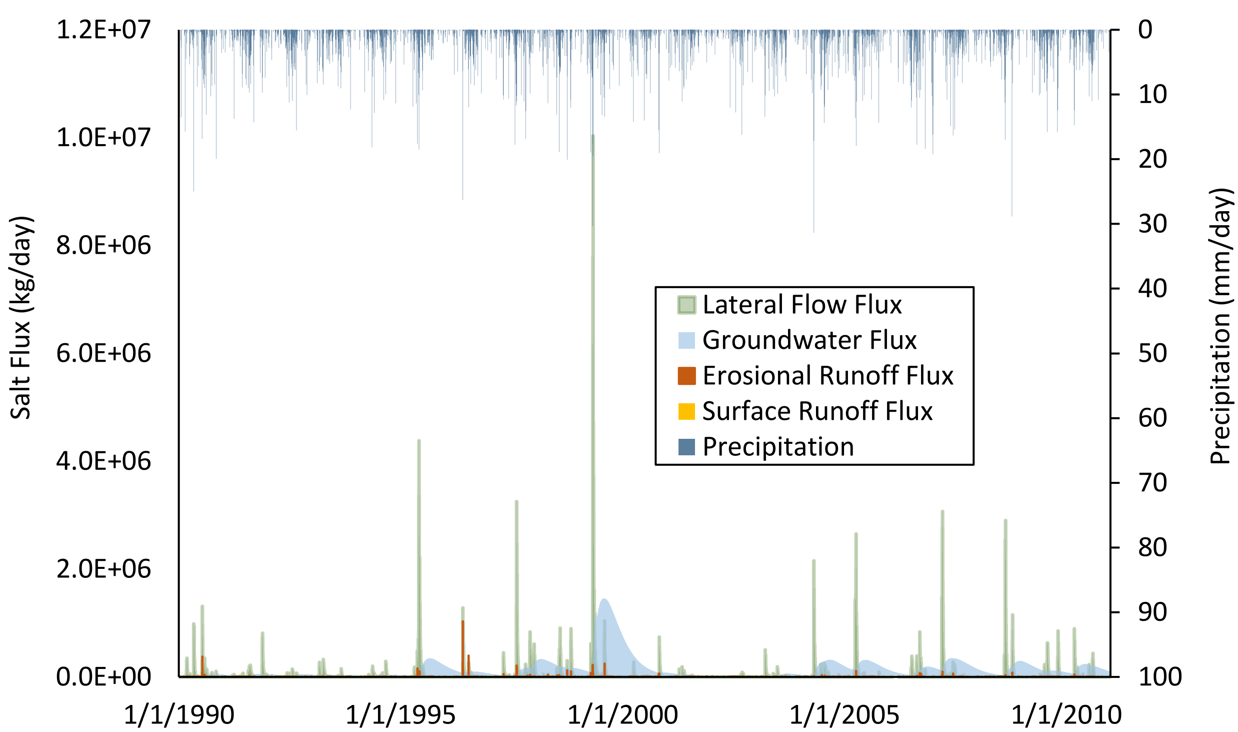

Figure 12- Time series of salt fluxes (kg/day) across the entire model period depicting the quick, intense pulses of soil lateral flow and consistency of groundwater salt export.

The modeled yearly salt mass exported was compared to the annual precipitation values. Zimmer (2021) anticipated there could be a relationship between these two variables with two years of field data, but a continuous model was needed to further evaluate the correlation. Predictions of future salt exports could benefit from a correlation between average annual precipitation and salt mass exported, but Figure 13 does not signify a strong linear correlation with the 20 years of historical data in this study (R^2=0.09). 1999 was an especially wet year for southeastern Colorado, while 2002-2003 was a period of drought. The salt mass exported from the Purgatoire River during 1999 was approximately 34 times larger than the salt mass exported in 2002 (Figure 14). However, the annual precipitation in 2006 was ~28 mm greater than the precipitation in 1995, but the salt mass exported in 1995 was more than 3 times the salt mass exported in 2006. These results do not indicate a firm relationship between annual precipitation and salt mass exports.

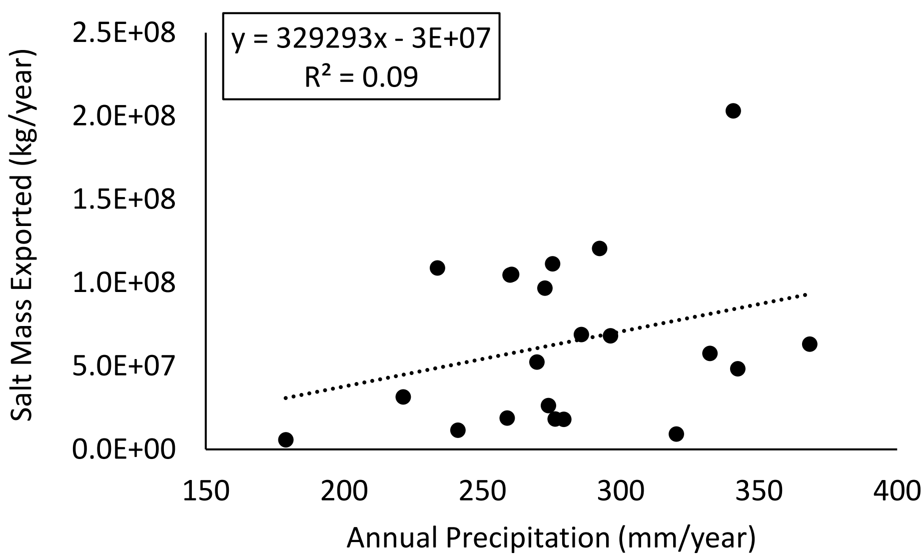

Figure 13- Modeled average annual salt exports from the Purgatoire River watershed (kg/year) vs the annual precipitation (mm/year).

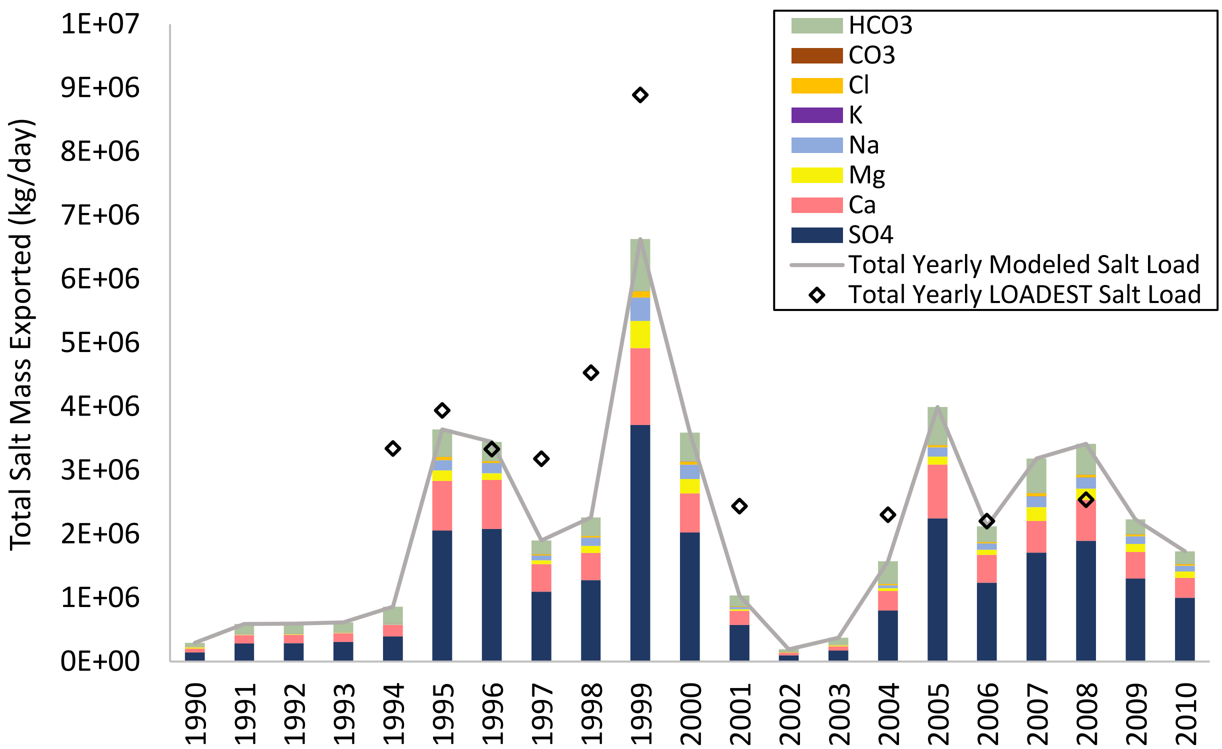

Figure 14- Total modeled annual salt exports from 1990-2010 broken down into the contribution of each ion and compared to LOADEST salt mass estimates.

SWAT-Salt results were used to visualize the spatial variation in subbasin salt exports across the Purgatoire River watershed. Comparing the maps to the mineral data presented in Figure 5, interestingly, the subbasins with the highest values of salt exports are not the subbasins with the highest mineral content. The northeastern subbasins of the watershed exports the largest quantities of salt mass per hectare through lateral flow and rainfall-runoff erosion (Figure 15). Groundwater salt exports are not as localized but are higher in upland subbasins as compared to the subbasins encompassing the Purgatoire main stem. This is likely due to the fact that the calibration parameter GWQMN, which is minimum depth of water to accumulate before groundwater return flow occurs, is slightly larger in the mainstem subbasins (606 mm) as compared to the rangeland subbasins (446 mm), (Table 2). Overall, there is not a region or group of subbasins that consistently export the largest amounts of salt through every flux pathway, highlighting the importance of both salt sources and hydrologic processes in governing salt loading to streams.

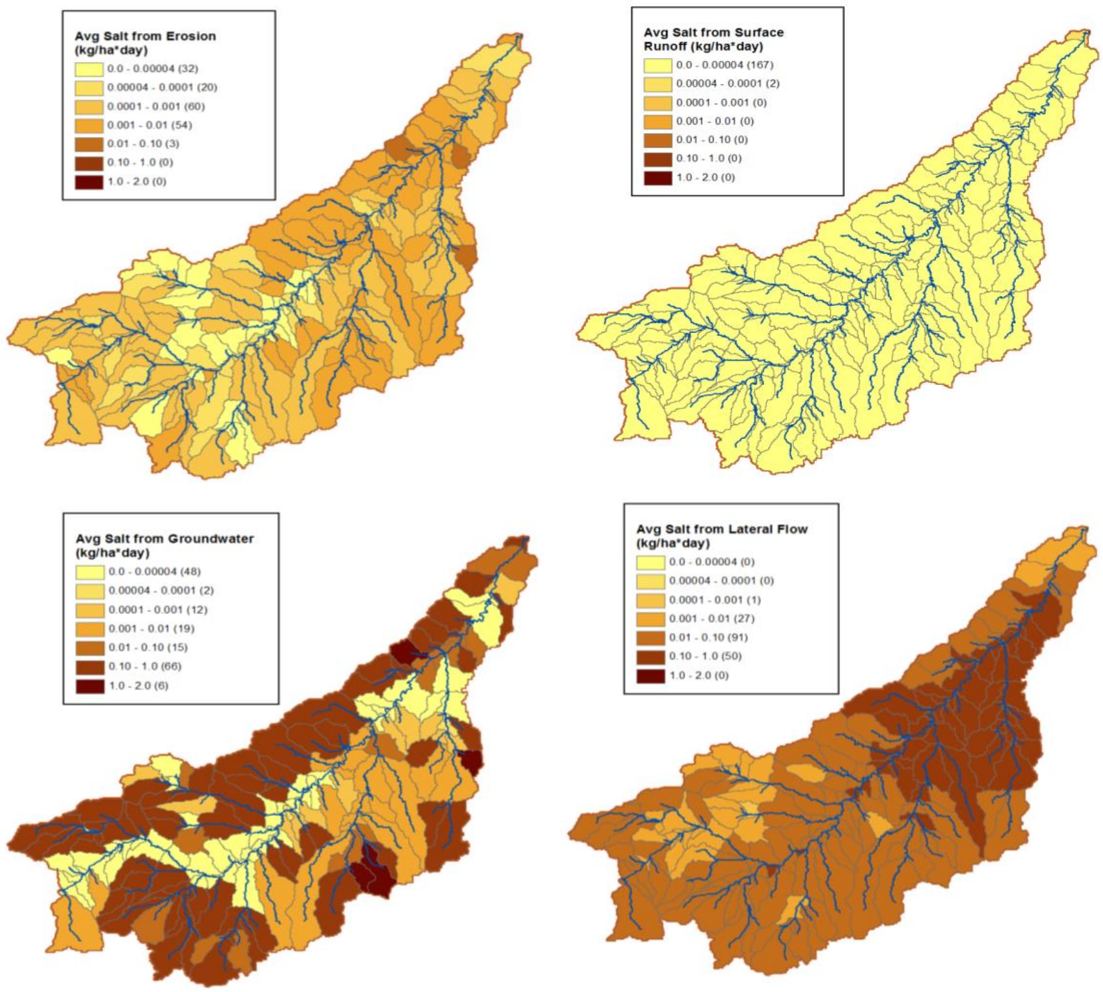

Figure 15- Subbasin averaged daily salt mass exports from each flux pathway (surface runoff, soil lateral flow, groundwater, and erosion rainfall-runoff) for the entire model period, 1990-2010.

3.3 Salt Mobilization, Transport, and Loading Under Climate Extremes

The 3 different scenarios of increasing storm intensity are referred to as scenarios 0-2. Scenario 0 is the baseline scenario with the downscaled PRISM daily precipitation data from 17 subbasins applied to the whole basin. Scenarios 1 and 2 incorporate increases in daily precipitation for any storm above 4 mm/day. All scenarios were run during the same historical period as the SWAT-Salt model, 1990-2010, and key findings are reported in Table 8. If the top ~5% of 24-hour rain events increase by the maximum predicted scenario, 35%, then the average yearly salt mass exported from the basin could increase by 73%. A 5% increase in 24-hour storm events is the average expected increase for Colorado based on all global climate models (Colorado Water Conservation Board, 2019), and this scenario could increase the average yearly salt exported from the basin by ~12%.

Table 8- Changes in salt mass loading for each of the 3 scenarios and percent of salt exported to stream due to each pathway.

	Average Salt Mass (kg/year)		*% of Total Landscape Mass Exports due to Each Pathway*			
Scenario	**Exported from Basin**	**% Increase from Baseline**	**Groundwater Flow**	**Soil Lateral Flow**	**Surface Runoff**	**Erosion Runoff**
0	7.0E7		78.2	21.4	0.0	0.4
1	7.8E7	12%	79.5	20.1	0.0	0.4
2	1.2E8	73%	82.8	15.9	0.0	1.3

The 4 flux pathways that provide salt to the stream (groundwater flow, soil lateral flow, surface runoff, and rainfall-runoff from erosion) were examined to determine if increasing precipitation intensity affects the relative contribution of each pathway on instream salt mass. Groundwater salt fluxes still dominate each scenario (Table 8), and increasing storm intensity appears to have a large effect on the magnitude of groundwater salt mass transport (Figure 16). The contributions of salt from each landscape flux pathway for Scenario 1, the 5% increase in precipitation intensity, is represented by the dotted lines in Figure 16. The first scenario increased the groundwater mass transported by 17.2%, and the second scenario increased the groundwater mass transported by over two orders of magnitude compared to the baseline scenario. Since the exports from the 4 flux pathways are much larger than the baseline scenario, Figure 15 does not display the relative contribution from each pathway of the total salt exported from the landscape in scenario 2. Also, it is important to note that the total salt exports from the landscape in scenario 2 are displayed on the secondary y-axis in Figure 15.

Soil lateral flow is the second largest source of salt, but the relative contribution of salt from soil lateral flow decreases with increasing precipitation intensity (Table 8). Surface runoff is the least relevant source of salt mass and also does not change much with increasing storm intensity. Runoff from rainfall-erosion events does not export salt to the stream on the same scale as groundwater and lateral flow fluxes, but this pathway becomes more relevant with increasing storm intensity. The relationship between increasing precipitation intensity and salt mass exported from erosional runoff could potentially be exponential, albeit the magnitude of erosional salt exports is still much smaller than groundwater exports (Table 8, Figure 16). Salt fluxes from erosional runoff increase dramatically with increasing precipitation intensity, however, the total yield is less than 1/100th of the mass exported through groundwater salt transport in each scenario (Table 8, Figure 16).

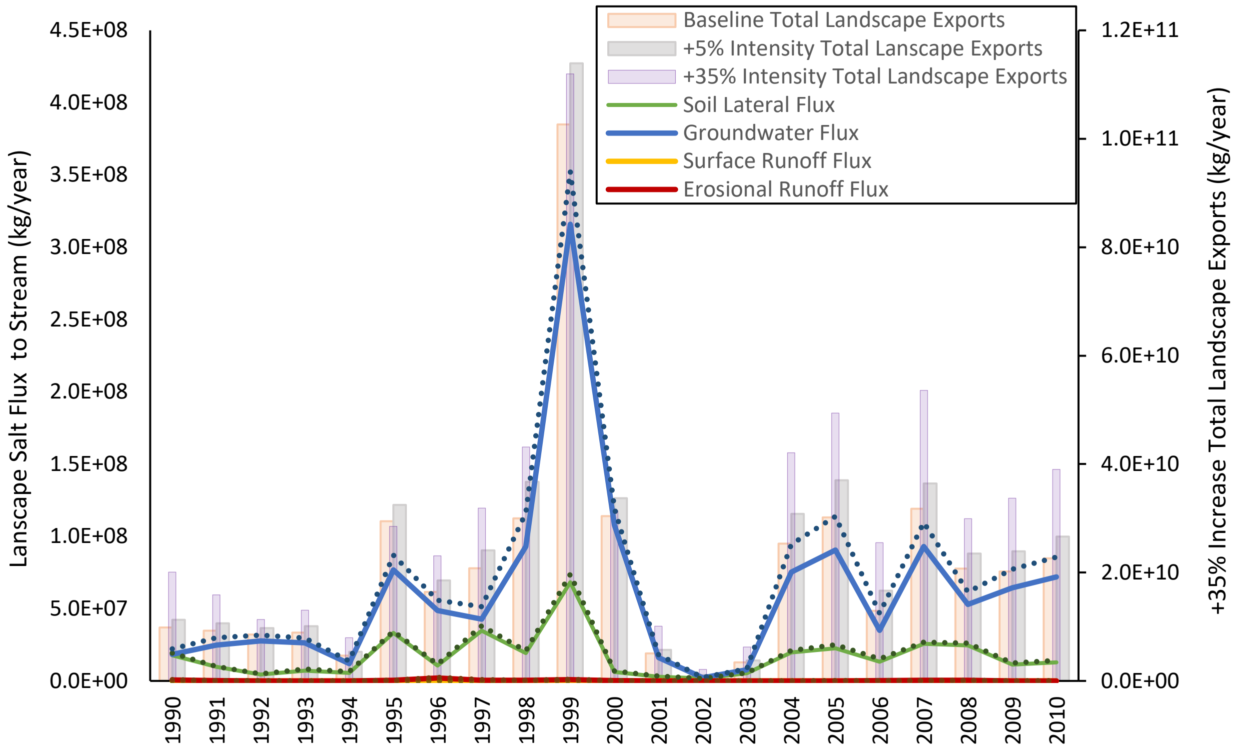

Figure 16- The annual total salt mass exported to the stream and the relative contributions of salt from the four flux pathways for scenarios 0 and 1 with the flux pathways from scenario 1 illustrated by dotted lines (primary y-axis). The secondary y-axis depicts the total salt exported from the landscape each year in scenario 2.

Lastly, the impact of increasing precipitation intensity was evaluated for an individual storm event. May of 1995 was a wet month, with over 78 mm of precipitation total, and a daily maximum of ~19 mm on May 30th, 1995. The time series of salt fluxes from May-July of 1995 is shown in Figure 17, where all 3 scenarios are compared. The baseline scenario is illustrated by the solid lines; Scenario 1 is illustrated by the thin dotted lines; and Scenario 2 is illustrated by the thick rectangular dotted lines. The colors depicting the salt flux pathways become darker with each sequential scenario number (i.e., the baseline scenario groundwater flux is the lightest blue, and scenario 2 is the darkest blue).

Compared to the baseline scenario, scenario 1 results in a 3.5% increase in the maximum daily pulse of salt mass (kg/day) from soil lateral flow on May 30th, 1995. However, scenario 2 results in a decrease in the maximum daily pulse of salt mass on the same day (Figure 17). The groundwater pulse has a greater delay time before reaching the stream and continues throughout the rest of calendar year. Increasing precipitation intensity does not change the pathways which govern salt transport in the Purgatoire River basin. Soil lateral flow controls salt transport from independent storm events, which is important over shorter periods (i.e., months or seasons), and groundwater fluxes govern salt transport over longer time periods (i.e., years or decades). The salt flux from rainfall-runoff erosion events becomes more significant in scenario 2, contributing 16.4% of the total salt flux during the storm event on May 20th, 1995 (Figure 17). This increase in salt mass leaving the landscape through erosion contributes to the decrease in the peak salt mass load from soil lateral flow.

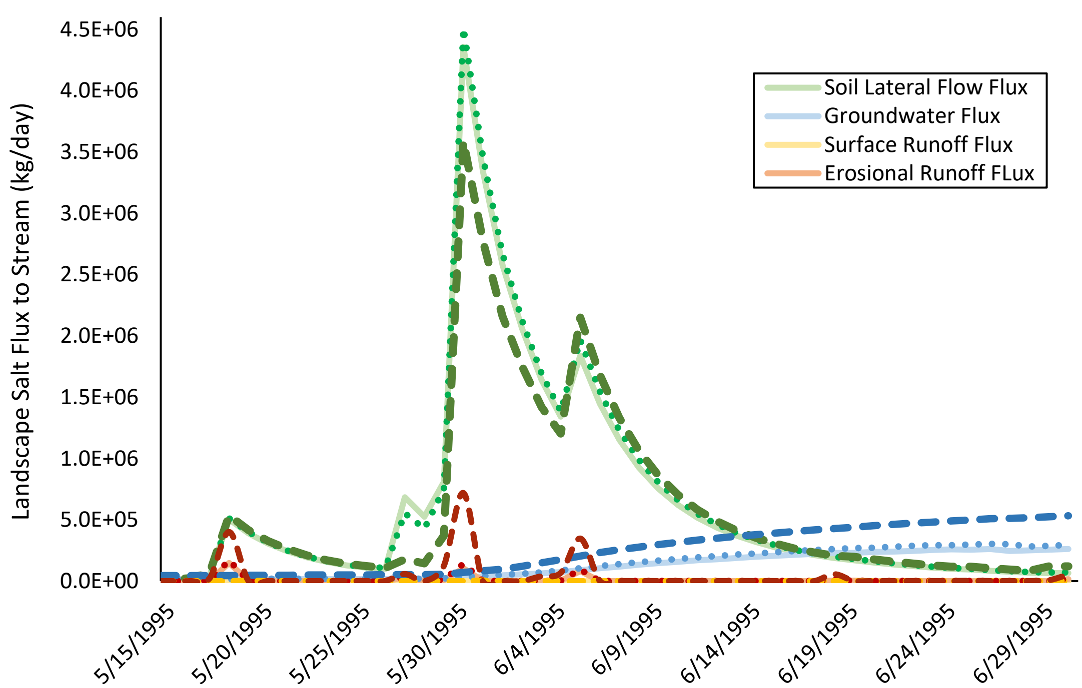

Figure 17- Hydrographs depicting the landscape response to a storm event. Solid lines represent the baseline scenario, thin dotted lines represent scenario 1, and thick, rectangular dotted lines represent scenario 3.

3.4 Limitations of Study

This study was limited in the data availability of initial salt concentrations in both the groundwater and soil profile; yet the mass of salt in the aquifer and soil profile appears to reach an equilibrium after ~5 model years. Two other input datasets also had increased uncertainty: precipitation data and reservoir inflow salt loads. Daily precipitation values were downscaled using regression equations from PRISM data due to the lack of reliable gage data in the watershed; and reservoir inflow salt loads were estimated through linear interpolation of daily specific conductance values and linear equations of specific conductance and ion concentration from a site upstream. This culmination of uncertainty in two important model inputs is a limitation of this study that could be improved with more reliable field measurements.

The SWAT model assumes land cover and land use remain constant throughout the model period of 1990-2010 using the input data from the National Land Cover Database (2011). Although the land cover and land use do not appear to change dramatically during this period, this assumption does not account for yearly differences in variables such as vegetation cover, amount of irrigated area, and cattle abundance, which could affect salt transport. This constant input parameter limited the results of the future scenarios of increasing precipitation intensity and could be better evaluated by manually inputting yearly changes in land use and land cover to the SWAT interface. The hydrologic balance will also be altered in the future with the loss of snowpack and snowmelt runoff due to increasing average temperatures. The impact of changes in snow hydrology on salt transport and loading in such regions should be further evaluated with climate change.

Another limitation of this study is the simplification of groundwater hydrology by SWAT. Since groundwater fluxes are important to both the hydrology and the salt mass transport in this watershed, future research could potentially incorporate groundwater modelling techniques with more spatial detail, such as MODFLOW. However, the SWAT groundwater modelling techniques are often deemed easier to apply because less detailed input data is required (e.g., groundwater table levels). This research suggests process-based models such as SWAT-Salt can be valuable in can be valuable in evaluating salt loadings from high-desert watersheds, particularly largely undeveloped landscapes without abundant water quality data.

4. SUMMARY AND CONCLUSIONS

4.1 Summary

This study developed a SWAT-Salt model for the Purgatoire River basin using SWAT input datasets, available historic water quality data, and downscaled PRISM precipitation data for the years 1990-2010. The modeled hydrology (1990-2021) reports satisfactory correlation statistics on the main stem of the Purgatoire River to USGS reported streamflow and shows correlation to the smaller arroyos in the watershed. The historic salt model developed in this study predicts that the Purgatoire River basin exported an average of ~64 million kg/year of salt between the years 1990-2020, with maximum and minimum values of ~202 million kg in 1999 and ~6 million kg in 2002. These values are similar to loads estimated by a previous study conducted in this watershed that used field measurements to estimate salt loads of ~62 million kg in 1990 and ~18 million kg in 2020 (Zimmer, 2021). The model presented in this study confirms that natural, undeveloped basins can export significant salt loads to downstream agricultural regions. We also conclude that the SWAT-Salt model developed in this study is a reasonable estimation of continuous yearly salt mass exports from the Purgatoire River watershed with limited input data.

The SWAT-Salt results match the temporal patterns of LOADEST estimated salt loads well. Average monthly loads of SO_4^{2-}, Ca^{2+}, Mg^{2+}, and HCO_3^- resulted in the best statistical correlations to LAODEST in the calibration period. These ions also have the greatest relative contributions to the total salt load, accounting for ~95% of the total salt exported from the Purgatoire River basin. The model determined that groundwater stream recharge is the greatest source of salt to the Purgatoire River, but soil lateral flow is the largest source of water to the river. This finding implies the groundwater salt concentration is greater than the soil water salt concentration.

The impact of increasing storm intensity as a result of climate change was evaluated through 3 different scenarios where the most extreme storms in the basin were increased in intensity (daily rainfall amounts) by 0%, 5%, and 35%. The maximum predicted scenario for Colorado based on global climate models is an 35% increase in intensity, which increases the salt transport in the Purgatoire River basin by 73% from the baseline scenario. The median expected scenario from global climate models is predicted to increase salt transport by ~12%, which is significant when the modeled annual average salt export is near ~64 million kg/year. Even as storm intensity increases, groundwater transport is the main pathway salt mass is exported to the stream, and salt transport due to surface runoff is largely negligible. Total salt exported from the landscape to the stream increased by two orders of magnitude in the most intense scenario compared to the baseline scenario. ~83 % of this mass increase is due to increases in groundwater export, 16% is due to increases in salt export from soil lateral flow, and 1.3% is due to increases in salt export from erosional runoff. The relative contributions of each salt flux pathway were similar for the two other scenarios evaluated. The influence of soil lateral flow slowly decreased, and the influence of erosional runoff slowly increased with increasing precipitation intensity. Overall, the SWAT-Salt model developed for the Purgatoire River basin provided a solid template for examining the impacts of changing precipitation intensity on salt export from a high desert watershed.

4.2 Key Findings

From this thesis, we conclude the following:

- The SWAT-Salt model developed estimated the Purgatoire River Watershed exported an annual average of ~64 million kg of salt each year from 1990-2010. Zimmer (2021) estimated that the total salt load in the Arkansas River after merging with the Purgatoire River was ~298 million kg in 1990 and ~161 million kg in 2020. This finding implies that largely undeveloped upland basins can export significant salt loads to downstream agricultural regions. Because of this, basin-wide programs for salt management must include processes in high-desert watersheds.
- Most of the salt mass is supplied to the Purgatoire River from the landscape through continuous groundwater exchange (~76% of total salt flux) and quick pulses of soil lateral flow during storm events (~24% of total salt flux).
- Future increasing storm intensity in semi-arid regions with changing climatic conditions can have a large impact on salt exports from high-desert landscapes. The average (5% increase) and maximum (35% increase) anticipated amplifications in rainfall intensity would result in 12% and 73% increases, respectively, in total salt mass (kg) exported from the Purgatoire River watershed during the 20 year period of 1990-2010.
- Process-based models such as SWAT-Salt can be valuable in evaluating salt loadings from high-desert watersheds and can be applied to other watersheds worldwide.

4.3 Future Work

Future work could utilize the model developed to evaluate other uncertainty scenarios, such as the impact of increasing temperatures and evapotranspiration rates in semi-arid regions. Other interesting work could predict changes in salt loads for extended periods into the future using downscaled global climate models. The opportunities to use this model for various climatic conditions are endless, as changing the weather input data (solar radiation, relative humidity, wind speed, temperature, and precipitation) in the SWAT interface is quite simple.

This study also provides a call for additional studies to further evaluate the relationship between average annual precipitation and salt mass exports, which could be crucial for water resource stakeholders. The lack of linear correlation between annual precipitation and salt mass exports in this study could have been caused by multiple factors. The impacts of increasing precipitation intensity presented in this paper demonstrate that the processes that govern salt transport are slightly altered during higher intensity storms (e.g., a decreased peak in salt mass transported from soil lateral flow, and an increase in salt mass transported from groundwater flow and rainfall-runoff erosion events). The lack of correlation in salt mass exported and average annual precipitation could demonstrate the timing and intensity of precipitation events is equally as important to salt mass exports as average annual precipitation depths.

Additionally, precipitation patterns can impact vegetation growth, which can subsequently impact salt movement from the landscape. After wet periods, vegetation would potentially grow more, and the increase in vegetation density on the landscape could impede salt transport. This phenomenon could cause a decrease in salt exports after longer wet periods. Alternatively, salt could potentially build up in the landscape during dry periods, so a less intense storm could generate increased salt exports after a dry period. Further research needs to consider the feedback loops between salt transport, average annual precipitation, precipitation intensity, and vegetation growth cycles.

If it is feasible, more intensive field data could improve similar studies. Manually taking groundwater and surface water samples more often could help validate the input parameters for the SWAT-Salt model, such as soil mineral content throughout the watershed and initial concentrations in the soil profile and aquifer. The groundwater hydrology could also be improved with more field data or a more detailed groundwater model interface, such as MODFLOW. Lastly, since hillslope can play a large factor in sediment yield and therefore salt yield in semi-arid catchments, any method to obtain a higher resolution DEM input dataset, such as LIDAR, should be attempted in future salt modeling of similar watersheds.

FUNDING ACKNOWLEDGEMENT

Financial support for this study was provided by National Science Foundation, Award No. 1845605.

REFERENCES

Abbaspour, K. C. (2012). *SWAT-CUP 2012: SWAT Calibration and Uncertainty Programs- A User Manual*.

Bailey, R. T., Tavakoli-Kivi, S., & Wei, X. (2019). A salinity module for SWAT to simulate salt ion fate and transport at the watershed scale. *Hydrology and Earth System Sciences*, *23*(7), 3155–3174. https://doi.org/10.5194/hess-23-3155-2019

Biggs, A. J. W., Silburn, D. M., & Power, R. E. (2013). Catchment salt balances in the Queensland Murray-Darling Basin, Australia. *Journal of Hydrology*, *500*, 104–113. https://doi.org/10.1016/j.jhydrol.2013.07.027

Burkhalter, J. P., Asce, M., & Gates, T. K. (2006). Evaluating Regional Solutions to Salinization and Waterlogging in an Irrigated River Valley. *Journal of Irrigation and Drainage Engineering*, *132*(1), 21–30. https://doi.org/10.1061/ASCE0733-94372006132:121

Cadaret, E. M., Nouwakpo, S. K., McGwire, K. C., Weltz, M. A., & Blank, R. R. (2016). Experimental investigation of the effect of vegetation on soil, sediment erosion, and salt transport processes in the Upper Colorado River Basin Mancos Shale formation, Price, Utah, USA. *Catena*, *147*, 650–662. https://doi.org/10.1016/j.catena.2016.08.024

Chang, X., Wang, S., Gao, Z., Chen, H., & Guan, X. (2021). Simulation of water and salt dynamics under different water-saving degrees using the sahysmod model. *Water (Switzerland)*, *13*(14). https://doi.org/10.3390/w13141939

Colorado Water Conservation Board. (2019). *Projecting Rainfall Intensity Duration Frequency Curves Under Climate Change*. https://waterinfo.org/wp-content/uploads/2020/02/CWCB-IDF-Curve-Projection-Paper-Final.pdf

Coumou, D., & Rahmstorf, S. (2012). A decade of weather extremes. In *Nature Climate Change* (Vol. 2, Issue 7, pp. 491–496). https://doi.org/10.1038/nclimate1452

Dugan, H. A., Bartlett, S. L., Burke, S. M., Doubek, J. P., Krivak-Tetley, F. E., Skaff, N. K., Summers, J. C., Farrell, K. J., Mccullough, I. M., Morales-Williams, A. M., Roberts, D. C., Ouyang, Z., Scordo, F., Hanson, P. C., & Weathers, K. C. (2017). Salting our freshwater lakes. *Proceedings of the National Academy of Sciences*, *114*(17), 4453–4458. https://doi.org/10.6073/pasta/455d73d4cb43514e503826211eba4e99

Duncan, R. A., Bethune, M. G., Thayalakumaran, T., Christen, E. W., & McMahon, T. A. (2008). Management of salt mobilisation in the irrigated landscape - A review of selected irrigation regions. In *Journal of Hydrology* (Vol. 351, Issues 1–2, pp. 238–252). https://doi.org/10.1016/j.jhydrol.2007.12.002

Foster, S., Pulido-Bosch, A., Vallejos, Á., Molina, L., Llop, A., & MacDonald, A. M. (2018). Impact of irrigated agriculture on groundwater-recharge salinity: a major sustainability concern in semi-arid regions. *Hydrogeology Journal*, *26*(8), 2781–2791. https://doi.org/10.1007/s10040-018-1830-2

Francis, David., & Hengeveld, H. Environment Canada. (1998). *Extreme weather and climate change*. Minister of the Environment. Catalog No. En57-27/1998-01E.

Gates, T. K., Burkhalter, P. J., Labadie, J. W., Valliant, J. C., & Broner, I. (2002). Monitoring and Modeling Flow and Salt Transport in a Salinity-Threatened Irrigated Valley. *Journal of Irrigation and Drainage Engineering*, *128*(2), 87–99. https://doi.org/10.1061/ASCE0733-94372002128:287

Gates, T. K., Garcia, L. A., & Labadie, J. W. (2006). *Toward Optimal Water Management in Colorado's Lower Arkansas River Valley: Monitoring and Modeling to Enhance Agriculture and Environment Colorado Agricultural Experiment Station*.

Georgakakos, A., Fleming, P., Dettinger, M., Peters-Lidard, C., Richmond, T. C., Reckhow, K., White, K., & Yates, D. (2014). *Ch. 3: Water Resources. Climate Change Impacts in the United States: The Third National Climate Assessment*. https://doi.org/10.7930/J0G44N6T

Hanson, B., Hopmans, J. W., & Šimůnek, J. (2008). Leaching with Subsurface Drip Irrigation under Saline, Shallow Groundwater Conditions. *Vadose Zone Journal*, *7*(2), 810–818. https://doi.org/10.2136/vzj2007.0053

Hassani, A., Azapagic, A., & Shokri, N. (2020). Predicting long-term dynamics of soil salinity and sodicity on a global scale. *Proceedings of the National Academy of Sciences*, *117*(52), 33017–33027. https://doi.org/10.1073/pnas.2013771117/-/DCSupplemental

Hegewisch, K. C., & Abatzoglou, J. T.*'Future Time Series' web tool. Climate Toolbox. (https://climatetoolbox.org/) accessed on 5/15/22*.

Hosseini, P., & Bailey, R. T. (2022). Investigating the controlling factors on salinity in soil, groundwater, and river water in a semi-arid agricultural watershed using SWAT-Salt. *Science of the Total Environment*, *810*. https://doi.org/10.1016/j.scitotenv.2021.152293

Jiang, J., Feng, S., Huo, Z., Zhao, Z., & Jia, B. (2011). Application of the SWAP model to simulate water-salt transport under deficit irrigation with saline water. *Mathematical and Computer Modelling*, *54*(3–4), 902–911. https://doi.org/10.1016/j.mcm.2010.11.014

Moriasi, D. N., Gitau, M. W., Pai, N., & Daggupati, P. (2015). Hydrologic and water quality models: Performance measures and evaluation criteria. *Transactions of the ASABE*, *58*(6), 1763–1785. https://doi.org/10.13031/trans.58.10715

Purgatoire Watershed Partnership. (2014). *Purgatoire River Watershed Plan*. doi:https://www.usbr.gov/watersmart/cwmp/docs/plans/Spanish-Peaks-Purtgatoire-Conservation-District.pdf

Reitz, M., Sanford, W. E., Senay, G. B., & Cazenas, J. (2017). Annual Estimates of Recharge, Quick-Flow Runoff, and Evapotranspiration for the Contiguous U.S. Using Empirical

Regression Equations. *Journal of the American Water Resources Association*, *53*(4), 961–983. https://doi.org/10.1111/1752-1688.12546

Schoups, G., Hopmans, J. W., Young, C. A., Vrugt, J. A., Wallender, W. W., Tanji, K. K., & Panday, S. (2005). Sustainability of irrigated agriculture in the San Joaquin Valley, California. *Proceedings of the National Academy of Sciences of the United States of America*, *102*(43), 15352–15356. https://doi.org/10.1073/pnas.0507723102

Šimůnek, J., Genuchten, M. Th., & Šejna, M. (2016). Recent Developments and Applications of the HYDRUS Computer Software Packages. *Vadose Zone Journal*, *15*(7), 1–25. https://doi.org/10.2136/vzj2016.04.0033

Stenson, M. P., Littleboy, M., & Gilfedder, M. (2011). Estimation of water and salt generation from unregulated upland catchments. *Environmental Modelling and Software*, *26*(11), 1268–1278. https://doi.org/10.1016/j.envsoft.2011.05.013

Tanji, K. K. (2004). *Salinity in the Soil Environment. In Salinity: Environment - Plants - Molecules* (A. Läuchli & U. Lüttge, Eds.). Kluwer Academic Publishers. doi:https://doi.org/10.1007/0-306-48155-3_2

Vengosh, A. (2014). Salinization and Saline Environments. *Treatise on Geochemistry (Second Edition)*, *11*, 325–378. http://dx.doi.org/10.1016/B978-0-08-095975-7.00909-8

Zamann, M., Shahidd, S. A., & Heng, L. (2018). *Guideline for Salinity Assessment, Mitigation and Adaptation Using Nuclear and Related Techniques*. SpringerOpen. https://doi.org/10.1007/978-3-319-96190-3

Zimmer, C., & Bailey, R. T. (2021). *Salt mobilization and transport in an upland desert catchment of the Lower Arkansas River Basin of Colorado* [Master of Science]. Colorado State University.

APPENDIX A

Table 9- Every USGS or DWE gage that is within the modeled section of the Purgatoire River watershed.

Gage Name	DWR Abbreviation	Reporting Start Date	Reporting End Date	Subbasin Number
Purgatoire River at Las Animas	PURLASCO	1/1/1922	Present	2
Purgatoire River Below Highland Dam	PURHILCO	1/1/2000	Present	8
Purgatoire River at Ninemile Dam Near Higbee	PURNICCO	10/1/1924	Present	18
Purgatoire River at Rock Crossing Near Timpas	PURRCKCO	6/1/1983	Present	28
Bent Canyon Creek at Mouth Near Timpas	BENTIMCO	10/1/1983	10/31/2020	32
Red Rock Canyon Creek at Mouth Near Thatcher	REDTHACO	5/26/1983	10/31/2020	43
Lockwood Canyon Creek Near Thatcher	LOCTHACO	4/21/1983	10/31/2020	49
Taylor Arroyo Below Rock Crossing near Thatcher	TAYBROCO	3/18/1983	10/31/2020	56
Purgatoire River near Thatcher	PURTHACO	7/1/1966	Present	81
Van Bremer Arroyo Near Model	VANMODCO	7/1/1966	Present	82
Purgatoire River at Fisher’s Crossing	PURFICCO	4/28/2010	Present	117
Purgatoire River Near Hoehne	PURHOECO	10/1/1954	Present	128
Purgatoire River at Trinidad	PURTRICO	10/1/1896	Present	142
Purgatoire River Below Trinidad Lake	PURBTRCO	1/1/1977	Present	141

APPENDIX B

Table 10- Every well sample recorded in the Purgatoire River watershed for the 8 salt ions.

		Ion Concentration (mg/L)							
USGS Site Number	**Sample Date**	**Ca^{2+}**	**Mg^{2+}**	**Na^{+}**	**K^{+}**	**Cl^{-}**	**SO_4^{2-}**	**HCO_3^{-}**	**CO_3^{2-}**
370909104341201	7/21/1981	62	17	140	3.6	12	150		
370908104342401	7/21/1981	2.3	0.2	260	1.2	14	63		
370931104350401	8/28/1981	90	22	220	6.4	160	250		
370746104374701	5/12/1979	14	85	1100	1.4	680	15		
372219103545501	12/27/1985	84	57	190	20	12	620		
372240103530201	5/11/1988	64	46	210	10	8.2	520		
	5/11/1988	57	40	220	9.9	10	490		
372344103524001	1/7/1986	120	110	200	9.2	76	2600		
372256103532301	8/14/1984	96	21	23	2.5	11	57		
	5/11/1988	92	22	25	2.4	13	72		
372638103494201	12/19/1985	460	230	770	2.8	330	3100		
373349103513001	2/6/1986	360	490	420	35	28	3600		
373208103490501	11/21/1984	450	360	310	21	56	2800		
373122103532501	8/9/1984	170	23	55	6.6	23	400		
372747103573001	5/11/1988	66	56	320	5	11	770		
372212104013101	9/24/1985	130	78	200	15	14	800		
372105104015801	2/5/1986	88	59	240	16	18	680		
372456104045401	6/14/1985			190		14	960		
372403104070601	11/20/1984	130		290	13	49	920		
372313104025801	8/14/1984				0				
372332104020001	8/7/1984	130	75	140	16	14	740		
373110104082201	5/11/1988	140	81	170	7	5.5	830		
380228103130701	8/19/1964			389		113	2020	288	0
380250103094001	8/19/1964			202		64	1020	180	0
380313103100801	8/19/1964			363		95	1880	202	0
380318103103401	4/26/1967	341	168	385	3.6	94	1860	454	0
# of Samples		21	20	25	22	25	25	4	4
Average Conc. (mg/L)		222	122	333	5.4	110	1171	281	0
St. Dev		133.9	124.5	227.9	8.5	144.1	1030.9	124.4	0

APPENDIX C

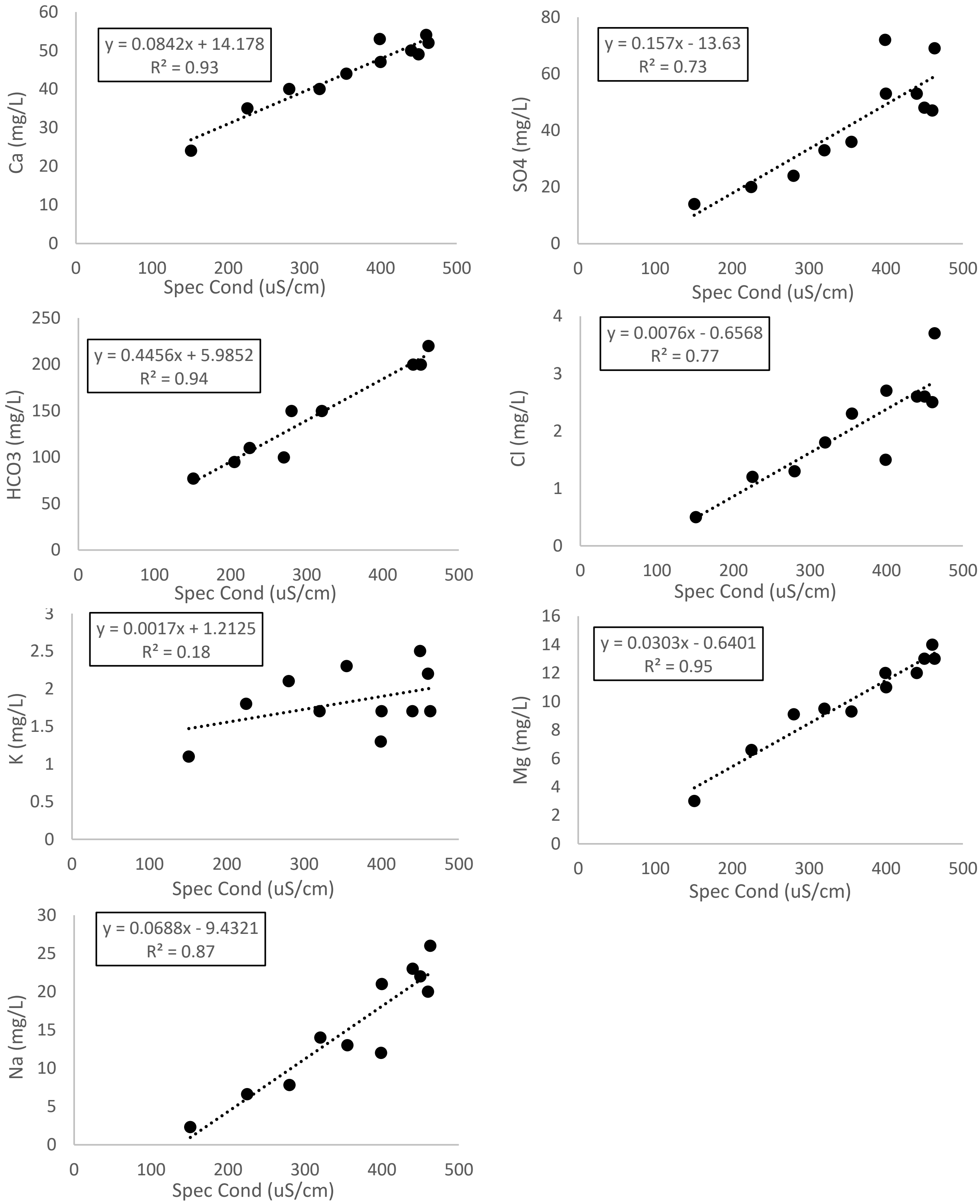

Figure 18- Regression equations between data obtained from the Purgatoire River at Madrid USGS site used to calculate daily salt ion loads from the reservoir with daily specific conductance data below the reservoir.

APPENDIX D

Table 11- The following regression equations were used in the LOADEST calculations of monthly ion loads. LOADEST automatically determines which equation is the best fit for each ion with the measured data.

Salt Ion	Regression Equation	AMLE R^2 (%)	BP (%)	NSE
HCO_3^-	$\ln(Load) = 9.9891 + (0.9575\ln(Q)) + (0.1254Sin(2pidtime)) + (0.0187Cos(2pidtime))$	99.19	1.15	0.98
Ca^{2+}	$\ln(Load) = 9.8588 + (0.8744\ln(Q)) + (-0.2210Sin(2pidtime)) + (-0.0419Cos(2pidtime)) + (-0.0023dtime)$	97.42	-1.79	0.98
Mg^{2+}	$\ln(Load) = 9.2662 + (0.8015\ln(Q)) + (-0.2730Sin(2pidtime)) + (-0.0164Cos(2pidtime)) + (0.0034dtime)$	94.98	2.79	0.96
Na^+	$\ln(Load) = 9.9575 + (0.7159\ln(Q)) + (0.1240Sin(2pidtime)) + (-0.2447Cos(2pidtime))$	94.39	-0.05	0.94
Cl^-	$\ln(Load) = 8.4164 + (0.6384\ln(Q)) + (-0.0268\ln(Q)^2) + (0.0819Sin(2pidtime)) + (-0.1095Cos(2pidtime))$	89.71	-7.70	0.76
K^+	$\ln(Load) = 5.9128 + (1.0119\ln(Q)) + (-0.0027dtime)$	98.83	3.96	0.96
SO_4^{2-}	$\ln(Load) = 11.6151 + (0.7732\ln(Q)) + (0.0315Sin(2pidtime)) + (-0.2752Cos(2pidtime))$	94.37	-1.55	0.95